

Online Research @ Cardiff

This is an Open Access document downloaded from ORCA, Cardiff University's institutional repository: <https://orca.cardiff.ac.uk/id/eprint/94846/>

This is the author's version of a work that was submitted to / accepted for publication.

Citation for final published version:

Andam-Akorful, S.A., Ferreira, V.G., Awange, J., Forootan, Ehsan ORCID: <https://orcid.org/0000-0003-3055-041X> and He, X.F. 2015. Multi-model and multi-sensor estimation of evapotranspiration over the Volta Basin, West Africa. International Journal of Climatology 35 (10) , pp. 3132-3145. 10.1002/joc.4198 file

Publishers page: <http://dx.doi.org/10.1002/joc.4198>
<<http://dx.doi.org/10.1002/joc.4198>>

Please note:

Changes made as a result of publishing processes such as copy-editing, formatting and page numbers may not be reflected in this version. For the definitive version of this publication, please refer to the published source. You are advised to consult the publisher's version if you wish to cite this paper.

This version is being made available in accordance with publisher policies.

See

<http://orca.cf.ac.uk/policies.html> for usage policies. Copyright and moral rights for publications made available in ORCA are retained by the copyright holders.



Multi-model and multi-sensor estimations of evapotranspiration over the Volta Basin, West Africa

International Journal of Climatology

Volume 35, Issue 10, pages 3132–3145, August 2015

The latest version can be found from

<http://onlinelibrary.wiley.com/doi/10.1002/joc.4198/abstract>

Please Cite

Andam-Akorful, S. A., Ferreira, V. G., Awange, J. L., Forootan, E. and He, X. F. (2015), Multi-model and multi-sensor estimations of evapotranspiration over the Volta Basin, West Africa. *Int. J. Climatol.*, 35: 3132–3145. doi: 10.1002/joc.4198

Multi-model and multi-sensor estimation of evapotranspiration over the Volta Basin, West Africa

S.A. Andam-Akorful^{a,b}, V.G. Ferreira^a, J.L. Awange^c, E. Forootan^d, X.F. He^a

^a*School of Earth Sciences and Engineering, Hohai University, Nanjing, China*

^b*Department of Geomatic Engineering, Kwame Nkrumah University of Science and Technology, Kumasi, Ghana*

^c*Western Australian Centre for Geodesy and the Institute for Geoscience Research, Curtin University, Perth, Australia*

^d*Institute of Geodesy and Geoinformation, Bonn University, Bonn, Germany*

Abstract

1 The estimation of large-scale evapotranspiration (ET) is complex, and typi-
2 cally relies on the outputs of land surface models (LSMs) or remote sensing
3 observations. However, over some regions of Africa, inconsistencies exist be-
4 tween different estimations of ET fluxes, which should be investigated. In
5 this study, we evaluate and combine different ET estimates from MODerate
6 resolution Imaging Spectroradiometer (MODIS), Global Land Data Assimi-
7 lation System (GLDAS), and terrestrial water budget (TWB) approach over
8 the Volta Basin, West Africa. ET estimates from water balance equation are
9 obtained as residuals from monthly terrestrial water-storage (TWS) changes
10 derived from Gravity Recovery and Climate Experiment (GRACE), Tropical
11 Rainfall Measurement Mission (TRMM)'s rainfall data, and in-situ discharge
12 from Akosombo Dam (Ghana). An averaged estimate of ET time series is
13 derived from all the ET estimations, under study, while taking into account
14 their uncertainties. The resulting ensemble averaged ET was then used to

Email address: vagnergf@hhu.edu.cn (V.G. Ferreira)

Preprint submitted to International Journal of Climatology

August 14, 2014

15 assess each of the individual ET estimates. Overall, out of the 7 investigated
 16 ET estimates (2 from the water balance approach of which one considers
 17 water storage using GRACE-derived TWS and the other ignoring it, 4 from
 18 GLDAS and 1 from MODIS), only MODIS (28.12 mm/month), GLDAS-
 19 NOAH (32.74 mm/month) and TWB (32.84 mm/month) were found to rep-
 20 resent the range of variability close to the computed averaged reference ET
 21 (30.25 mm/month). ET estimations inferred from MODIS were also found
 22 to represent relatively lower magnitude of uncertainties, i.e., 3.99 mm/month
 23 over the Volta Basin (cf. 7.06 and 18.85 mm/month for GLDAS-NOAH and
 24 TWB-based ET estimations, respectively).

Keywords: Evapotranspiration, GLDAS, GRACE, MODIS, terrestrial
 water-storage changes, TRMM, Volta Basin

25 **1. Introduction**

26 Evapotranspiration (ET) represents the sum of evaporation and plant
 27 transpiration from the Earth’s land and ocean surface to the atmosphere,
 28 which makes it an important hydrological component to relate the water,
 29 energy, and carbon cycles ([Alton et al., 2009](#)). ET is identified as the major
 30 factor that determines groundwater recharge and surface runoff; two critical
 31 components of available water storage ([Komatsu et al., 2008](#)). Observing the
 32 variability of ET is vital for many regions, such as the Lake Volta basin in
 33 West Africa, since its dynamic reflects the atmosphere-hydrosphere-biosphere
 34 interactions over the region ([Fisher et al., 2011](#); [Jung et al., 2010](#)). In fact,
 35 ET accounts for approximately 90% of precipitation in the Volta River basin
 36 of West Africa ([Andreini et al., 2000](#)). In addition, estimation of ET over

the Volta Basin is necessary owing to its vulnerable response under global warming (Oguntunde et al., 2006). Several studies, e.g., Lebel et al. (2000); Kasei et al. (2009); Oyebande & Odunuga (2010); Nicholson (2013) indicated that the whole West African sub-regions (including the Volta Basin) have experienced reduced rainfall amounts since the 1970s, which most likely coincided with the observed rising global temperature, leading to the last decade drought.

The intensification of agriculture in West Africa leads to a change in surface and subsurface characteristics, which directly affects ET rates (Kunstmann & Jung, 2007) that, in turn, could affect the regional rainfall patterns. For the Volta Basin, for example, the influence of climate variability and change has been shown by Jung & Kunstmann (2007) to account for a spatial mean increase of 5% (~ 45 mm) of mean annual change in rainfall. **Weaker change in the precipitation than in the rainfall, infiltration excess change exceeds the precipitation change, revealing a highly nonlinear relationship (e.g., Jung & Kunstmann, 2007).** Under the influence of climate change, Neumann et al. (2007) reported positive and negative trends in temperature and precipitation respectively within the basin. This phenomenon could lead to the occurrence of dry periods due to possibly increased ET rates and reduced precipitation. Being one of the most vulnerable agricultural factors to climate change, understanding ET patterns in the basin is therefore crucial to food security and the general socio-economic health of the region (see, e.g., Estes et al., 2013; Kousari & Ahani, 2012).

Despite being a critical hydrological variable, direct measurement of ET

62 is difficult especially in large basins such as the Volta (Su, 2002). Routine
 63 monitoring of ET requires a dense distribution of hydro-meteorological sta-
 64 tions with long-term data records (e.g., temperature, wind patterns, rain,
 65 solar radiation, humidity, precipitation, etc.). In the Volta Basin, such
 66 hydro-meteorological stations are sparsely distributed (Adjei et al., 2012;
 67 Opoku-Duah et al., 2008), necessitating the use of remotely sensed data and
 68 hydrological models as alternative means for estimating ET and other hydro-
 69 logical quantities. Previous methods employed to obtain ET estimates over
 70 the basin include the Surface Energy Balance Algorithm for Land (SEBAL)
 71 (see, e.g., Hendrickx et al., 2006; Hafeez et al., 2007; Opoku-Duah et al.,
 72 2008; Compaoré et al., 2008) and the Advection-Aridity relationship model
 73 (Oguntunde, 2004). SEBAL has an advantage that it can be applied with-
 74 out using ground measurements, and has demonstrated potential in mapping
 75 ET worldwide (Bastiaanssen et al., 1998). Other option, for example, could
 76 be the satellite-based energy balance based on Mapping Evapotranspiration
 77 with Internalized Calibration (METRIC) procedure for calculating ET (see,
 78 e.g., Allen et al., 2007; Santos et al., 2008; Pôças et al., 2013).

79 Opoku-Duah et al. (2008), for instance, found that MODerate resolution
 80 Imaging Spectroradiometer (MODIS) driven by SEBAL evapotranspiration
 81 estimates under-performed by up to 2 mm/day against point observations
 82 such as eddy correlation, and the Penman-Monteith method. Spatial scale
 83 mismatch was reported to be the main reason for the obtained inconsistency.
 84 Compaoré et al. (2008) used SEBAL to map evaporation in the White Volta
 85 sub-basin, at the begin and end of a dry season using Landsat and MODIS
 86 images, and established that SEBAL had potential for mapping ET over

87 tropical areas. [Schüttemeyer et al. \(2007\)](#) used the modified Makkink for-
 88 mula by considering incoming solar radiation obtained from Meteorological
 89 Satellite (Meteosat) data and the green vegetation fraction using enhanced
 90 vegetation index from MODIS. They reported daily mean errors ranging from
 91 5% to 35% of measured ET and a seasonal error smaller than 5% over the
 92 Volta Basin.

93 At a global scale, model data such as those of Global Land Data Assimila-
 94 tion System (GLDAS) ([Rodell et al., 2004b](#)) and MODIS Global Evapotran-
 95 spiration Project (MOD16) ([Mu et al., 2013](#)) are important sources that can
 96 also be applied at regional scale, e.g., over the Volta Basin to infer on ET.
 97 Their uncertainties and validity for the basin are, however, unknown. It is
 98 therefore vital to validate them using independent approaches, e.g., terrestrial
 99 water budget (TWB) approach ([Rodell et al., 2004a, 2011](#); [Xue et al., 2013](#);
 100 [Zeng et al., 2014](#)). Based on the principle of mass conservation, one can use
 101 independently derived components of the hydrological cycle to estimate ET.
 102 Until recently, application of the water balance approach was limited due
 103 to limited accessibility to direct measurements of terrestrial water-storage
 104 component, especially over large areas. With the launch of the Gravity Re-
 105 covery and Climate Experiment (GRACE) satellite mission in 2002 ([Tapley](#)
 106 [et al., 2004](#)), however, quantification of total water-storage (TWS) and its
 107 changes is now possible ([Cazenave & Chen, 2010](#)). The TWB approach,
 108 which considers GRACE-based TWS changes has been used as an alterna-
 109 tive method for estimating ET as residuals (see, e.g., [Rodell et al., 2004a](#);
 110 [Ramillien et al., 2006](#); [Boronina & Ramillien, 2008](#); [Cesanelli & Guarracino,](#)
 111 [2011](#); [Moiwo et al., 2011](#); [Sahoo et al., 2011](#); [Rodell et al., 2011](#); [Long et al.,](#)

112 2014; Zeng et al., 2014).

113 For instance, Rodell et al. (2004a) indicated that TWB-based ET esti-
114 mates agreed well with those provided by the European Center for Medium
115 range Weather Forecasting (ECMWF) and the Global Land Data Assimila-
116 tion System (GLDAS) over Mississippi River Basin with root-mean-square-
117 error (RMSE) of 19.50 and 24.90 mm/month, respectively. Ramillien et al.
118 (2006) achieved similar results to those of Rodell et al. (2004a) over 16 se-
119 lected river basins and showed that GRACE-derived ET estimates were com-
120 parable to those of global land surface models (LSM), namely: Land Dynam-
121 ics Model (LaD), Organising Carbon and Hydrology in Dynamic Ecosystems
122 (ORCHIDEE), GLDAS, and a conceptual WaterGap Hydrological Model
123 (WGHM) model. Across West Africa, only a few GRACE applications have
124 been carried out, with emphasis on the Niger Basin and the Sahel region
125 (see, e.g., Grippa et al., 2011; Boy et al., 2012; Hinderer et al., 2012) and on
126 basins in Sub-Saharan Africa (e.g., Xie et al., 2012). Grippa et al. (2011)
127 showed that GRACE data can reproduce TWS inter-annual variability over
128 the Sahel region. Xie et al. (2012) used seven years of GRACE data to cali-
129 brate a semi-distributed regional scale hydrological model, the soil and water
130 assessment tool (SWAT). A statistical approach to predict GRACE-derived
131 total water storage in relation to the major teleconnections and precipitation
132 changes in West Africa is addressed in Forootan et al. (2014b). However, to
133 the best of our knowledge, the estimation of TWB-based ET over the Volta
134 Basin has not been carried out in the previous studies.

135 Recently, Zeng et al. (2014) implemented the TWB method to evaluate
136 the estimated global monthly ET through coupling water balance model with

137 a machine learning algorithm. They found that the water balance learning
 138 machine based ET agreed with a RMSE of 26.7 mm/month, while MOD16
 139 ET products (Mu et al., 2013) presented a RMSE of 34.32 mm/month against
 140 ET estimated from water balance approach. Recently, Long et al. (2014)
 141 assessed the uncertainties in ET output of North American Land Data As-
 142 simulation System (NLDAS)’s models (Mitchell et al., 2004), two remote
 143 sensing-based products (MODIS and AVHRR) and GRACE-inferred ET us-
 144 ing the “three-cornered hat” method, and found the relative uncertainties in
 145 ET to be moderate in MODIS– and AVHRR-based ET (10–15 mm/month),
 146 and highest in GRACE-inferred ET (20–30 mm/month) without *a priori*
 147 knowledge of the true value of ET.

148 As a contribution to the estimation of ET over the data scarce Volta
 149 Basin, this study aims at (i) evaluating ET estimates over the Volta Basin
 150 from four existing GLDAS-simulations of Variable Infiltration Capacity (VIC)
 151 (Liang et al., 1994), NOAH (Ek et al., 2003), MOSAIC (Koster & Suarez,
 152 1996), Community Land Model (CLM) (Dai et al., 2003), those derived from
 153 MODIS (Mu et al., 2013), and the water balance approach, and (ii) once
 154 the time series of ET estimations and their uncertainties have been deter-
 155 mined using the three-cornered hat method (Long et al., 2014, e.g.), they are
 156 used to generate an ensemble-averaged ET estimation over the Volta Basin,
 157 which is adopted as a reference in this study to access uncertainties of various
 158 approaches under investigation. To use the water budget equation, precipi-
 159 tation data from the Tropical Rainfall Measuring Mission (TRMM) and the
 160 observed discharge from the Akosombo Dam in Ghana have been included.

161 2. Study Area

162 2.1. Geography

163 The Volta Basin, located at the semi-arid West African savanna zone, has
164 its water resources shared amongst six riparian countries namely; Ghana,
165 Burkina Faso, Mali, Ivory Coast, Togo and Benin (Fig. 1), and drains a total
166 area of about 417,382 km² (van Zwieten et al., 2011). The topography is
167 mostly flat and elevations do not exceed 1000 m in most parts. The Volta
168 River has three main tributaries – the Black Volta, White Volta and Red
169 Volta, and drains into the Gulf of Guinea and Atlantic Ocean completing a
170 journey of about 1,200 km (Shahin, 2002). Lake Volta is one of the most
171 important physiographic features in Ghana with a submerged area of 8,500
172 km² (Oguntunde et al., 2006). It is the largest man-made lake in the world
173 extending from the Akosombo Dam in southeastern Ghana to approximately
174 400 km to the north (Shahin, 2002). It is fed by numerous tributary rivers
175 to the Volta River; thus, the volume of water in the reservoir and the area
176 shrinks during dry seasons and swells during the rainy seasons (Tanaka et al.,
177 2002).

178 [Figure 1 around here.]

179 Volta Basin has an estimated population of over 20 million people with a
180 growth rate of 3% per year, which relies on its water resources (Kasei et al.,
181 2009). Additionally, Opoku-Duah et al. (2008) reported that over 70 million
182 people of West Africa depend on the Volta Basin for food, water resources,
183 housing and transport. A large number of dams and reservoirs have been con-
184 structed within the basin for irrigation, domestic, power generation, fisheries,

185 and industrial purposes (see, e.g., [Leemhuis et al., 2009](#); [van Zwieten et al.,](#)
186 [2011](#)), posing threats to sustainable water resource management. Efficient
187 management of water resources within the basin, therefore, is of extreme
188 importance for socio-economic development of the region. This calls for reg-
189 ular monitoring of its hydrological variables, and their consequent impacts
190 on water resources to ensure a sustainable use.

191 2.2. *Climate*

192 The basin’s climate is mainly governed by the southwestern monsoon
193 and the northeastern trade winds (*harmattan*), which exhibits a north-south
194 gradient. The climatic gradient results in differing climatic conditions in the
195 southern and northern sections of the basin as evidenced by the unimodal and
196 bimodal rainfall regimes in the north and south respectively ([Sultan et al.,](#)
197 [2005](#)). Farmers in the basin have widely reported the delays in the onset
198 of rainy seasons over the past several decades ([van de Giesen et al., 2010](#)).
199 [Jung & Kunstmann \(2007\)](#), using a simulated scenario, reported a delay
200 in the onset of rainy seasons, with an increase in inter-annual precipitation
201 variability over the Volta Basin as a consequence of global climate change. In
202 addition, it experiences extreme climatic conditions, and is highly vulnerable
203 to droughts and floods (cf., [van de Giesen et al., 2010](#); [Taylor et al., 2006](#);
204 [Samimi et al., 2012](#)).

205 Annual precipitation rates decrease from 1,200–1,500 mm/year in the
206 coastal south to 300–500 mm/year in the Sahelian north. The semi-arid
207 regions have variable rainfall patterns with extreme cases of droughts and
208 sporadic floods and has an annual average rainfall between 1,150 mm in the
209 north and 1,380 mm in the south. [Owusu et al. \(2008\)](#) reported that the El

210 Niño Southern Oscillation (ENSO) teleconnection patterns induce extreme
 211 precipitation events in the basin. Consequently, recent droughts and floods
 212 have largely been coincident with El Niño/La Niña events. Temperatures
 213 vary between approximately 16°C and 40°C depending on the season, time
 214 of day, and elevation (Oguntunde et al., 2006), with an average air temper-
 215 ature of approximately 27.8°C. Jung & Kunstmann (2007) reported a mean
 216 annual temperature increase of 1.2–1.3°C based on regional climate simu-
 217 lations. The mean relative humidity rises up to about 80% in September
 218 and falls to about 20% in January (Gyau-Boakye & Tumbulto, 2000). Fo-
 219 rootan et al. (2014b) showed that using the statistical relationships between
 220 precipitation and water storage changes, forced by sea surface temperature
 221 patterns, one can fairly predict the main annual and inter-annual variability
 222 of water storage over West Africa.

223 **3. Methods and Data**

224 To perform an inter-comparison among ET estimates, several datasets
 225 have been used. In Section 3.1, a summary of the main products is presented
 226 while in Section 3.2, the methods of ET estimations are discussed.

227 *3.1. Datasets*

228 The time span of the all dataset applied in this study (i.e., GRACE,
 229 TRMM, GLDAS, MODIS, in-situ discharge and atmospheric water storage
 230 dataset from ERA-Interim) cover a period from January 2003 to December
 231 2012 due to data overlap in that time span.

232 3.1.1. GRACE Level 2 Products

233 The Release-05 (RL05) Level 2 products (L2) as described in Bettadpur
234 (2012a,b), i.e., potential spherical harmonic coefficients (i.e., Stokes’s coef-
235 ficients) used in this study were derived from three official processing cen-
236 ters: Center for Space Research (CSR), University of Texas; Jet Propulsion
237 Laboratory (JPL); the GeoForschungsZentrum (GFZ), available at [ftp://](ftp://podaac-ftp.jpl.nasa.gov/allData/grace/L2/)
238 [podaac-ftp.jpl.nasa.gov/allData/grace/L2/](ftp://podaac-ftp.jpl.nasa.gov/allData/grace/L2/). Additionally, water stor-
239 age changes derived from climatological data (cf. sections 3.1.6 and 3.2.2)
240 were used to independently assess the quality of GRACE-derived water-
241 storage changes over the Volta Basin. Data from these three centers were
242 used due to their unique processing procedures that yield different terrestrial
243 water-storage anomalies (e.g., Bruinsma et al., 2010; Klees et al., 2008). The
244 time span of the dataset covered the period from January 2003 to December
245 2012, with the data for June, 2003, January and June of 2011, and May and
246 October of 2012 missing. These missing GRACE derived terrestrial water-
247 storage anomalies were estimated using the previous and the next month’s
248 (e.g., Ramillien et al., 2006). Cross-validation (not presented here) shows
249 that this method presents a RMSE of 19.69 mm/month.

250 Because GRACE alone cannot directly provide degree one Stokes’s coef-
251 ficients ($C_{1,0}$, $C_{1,1}$ and $S_{1,1}$), which represent the changes in the geocenter
252 due to mass redistribution in the Earth system, they were replaced by values
253 from the results provided by Swenson et al. (2008) to improve estimates of
254 mass variability. Including these coefficients would represent impacts on the
255 amplitude of the annual and semi-annual GRACE-derived water storage esti-
256 mations. The zonal degree two coefficients ($C_{2,0}$) were replaced by the values

257 derived from Satellite Laser Ranging (SLR) (Cheng & Tapley, 2004; Cheng
 258 et al., 2013) because GRACE-derived $C_{2,0}$ coefficients present relatively high
 259 uncertainties. The secular decrease in $C_{2,0}$ resulted primarily due to glacial
 260 isostatic adjustment, and is modulated by ocean and ice mass redistribution
 261 (e.g., Cox & Chao, 2002). The processing scheme is provided in section 3.2.1.

262 3.1.2. Tropical Rainfall Measuring Mission (TRMM)

263 TRMM is a joint mission between the United States (NASA) and Japan
 264 (Japan Aerospace Exploration Agency) (Huffman et al., 2007). TRMM is
 265 designed to monitor tropical rainfall in the latitude range $\pm 50^\circ$. In this work,
 266 we used monthly averaged 3B43 V7 rainfall rate products with a spatial re-
 267 solution of 0.25° (e.g., Fleming & Awange, 2013), which are inferred from
 268 not only the TRMM observations, but also employs data from a number of
 269 other satellites and ground-based rain gauge data (Huffman et al., 2007).
 270 The data was obtained from NASA’s Goddard Earth Sciences and Data
 271 and Information Service Center (GES DISC) available at [http://mirador.](http://mirador.gsfc.nasa.gov/)
 272 [gsfc.nasa.gov/](http://mirador.gsfc.nasa.gov/). TRMM observations have been used in several studies of
 273 rainfall over Africa (e.g., Nicholson et al., 2003; Adeyewa & Nakamura, 2003)
 274 and specifically over the Volta Basin (e.g., Adjei et al., 2012; Thiemig et al.,
 275 2012, 2013). Adjei et al. (2012) reported that there is the tendency of TRMM
 276 to underestimate rainfall in the Black Volta sub-basin especially in the wet
 277 season. In addition, Thiemig et al. (2013) reported that TRMM captures the
 278 intra-seasonal variability, the spatial distribution pattern, the average annual
 279 precipitation, and the timing of the highest annual precipitation event well
 280 over Volta Basin. Thiemig et al. (2012) found that interpolated rainfall
 281 derived from ground observations agrees well with TRMM, exhibiting only a

282 slight underestimation of 11%.

283 3.1.3. *Global Land Data Assimilation (GLDAS)*

284 GLDAS is a global hydrological model that generates a series of global
285 land surface state (e.g., soil moisture, snow water equivalent, surface temper-
286 ature) and flux (e.g., evapotranspiration and sensible heat flux), e.g., Rodell
287 et al. (2004b). It incorporates both ground- and space-based observation
288 systems to produce optimal estimates of land surface state of flux. Four
289 products, namely: MOSAIC, NOAH, CLM and VIC simulate GLDAS's hy-
290 drological fields. Hence, the total ET field which is the sum of transpiration
291 from vegetation and surface evaporation with a spatial resolution of 1° was
292 used. The GLDAS data were retrieved from [http://disc.sci.gsfc.nasa.](http://disc.sci.gsfc.nasa.gov/hydrology/data-holdings)
293 [gov/hydrology/data-holdings](http://disc.sci.gsfc.nasa.gov/hydrology/data-holdings).

294 3.1.4. *MODIS Global Evapotranspiration Project (MOD16)*

295 The MOD16 global ET data is provided by Earth Observing System
296 of the National Aeronautics and Space Administration (NASA/EOS) as
297 part of global ET project, and are available at [http://www.ntsg.umd.edu/](http://www.ntsg.umd.edu/project/mod16)
298 [project/mod16](http://www.ntsg.umd.edu/project/mod16). The estimates are derived from MODIS-based vapor pres-
299 sure deficit, solar radiation and air temperature, as well as a network of eddy
300 towers and global meteorological data (Cleugh et al., 2007; Mu et al., 2011).
301 The MOD16 algorithm in Mu et al. (2011) is based on an improved version
302 of Mu et al. (2007), which is also based on the Penman-Monteith equation,
303 Monteith (1965). The MODIS data (i.e. MOD16) is available at 8-day,
304 monthly, and annual intervals. Analysis for this study is based on monthly
305 products with a spatial resolution of 0.5° .

306 3.1.5. *In-situ discharge*

307 In addition to the satellite- and model- derived datasets, monthly dis-
308 charge rates from Akosombo Dam (cf. Fig. 1) were also used to estimate
309 ET using the water balance approach (section 3.2.2). The data was obtained
310 from the Water Research Institute of Ghana covering the the time span from
311 February 2003 to December 2012 and the records are complete. Before the
312 construction of the Akosombo Dam in 1964, the river flow was extremely
313 irregular as one can see by inspecting Fig. 9.4 of (Shahin, 2002, p. 394) that
314 shows the discharge observed at the Senchi hydrological station (downstream
315 of Akosombo Dam). The filling of the Volta Lake took four years (1964-68)
316 after the completion of the dam construction and since then, Volta Lake
317 has helped to stabilize the out flow reaching the most downstream and key
318 station at Senchi (Shahin, 2002, p. 394).

319 3.1.6. *Precipitable water and vapor flux divergence*

320 The specific humidity (q), the eastern (u), and the northern (v) di-
321 rection winds from ERA-Interim (Dee et al., 2011), the latest global at-
322 mospheric reanalysis produced by the European Centre for Medium-Range
323 Weather Forecasts (ECMWF), were used to calculate the vapor flux di-
324 vergence $\nabla \cdot \mathbf{Q}$ and precipitable water W in Eqs. (2) and (5) of Yirdaw
325 et al. (2008), respectively. They are used in this study with a spatial resolu-
326 tion of 1° in order to check the GRACE-derived water-storage changes (see
327 sub-section 3.2.2). The data were retrieved from [http://apps.ecmwf.int/](http://apps.ecmwf.int/datasets/data/interim_full_daily/)
328 [datasets/data/interim_full_daily/](http://apps.ecmwf.int/datasets/data/interim_full_daily/).

329 3.2. Methods

330 3.2.1. Computation of GRACE-derived water-storage changes

331 Monthly GRACE derived gravity coefficients exhibit correlated errors and
332 short-wavelength noises that manifest themselves as stripes in the spatial
333 maps of terrestrial water-storage anomalies (Swenson & Wahr, 2006). We
334 removed the stripes using a de-correlation filter known as the P4M6 filter
335 scheme proposed by Chen et al. (2010), which is a variation of the method
336 described in Swenson & Wahr (2006). An exhaustive comparison of the
337 suitability of the filter methods available can be found, e.g., in Werth et al.
338 (2009) and Duan et al. (2009). For spherical harmonic coefficients of orders
339 6 and above, a degree 4 polynomial was fitted by least squares and removed
340 from even and odd coefficient pairs (Chen et al., 2010; Swenson & Wahr,
341 2006). The resulting de-stripped terrestrial water-storage anomalies, which
342 still contained some inherent errors, were smoothed using a Gaussian filter
343 with half-width radius of 300 km (half-width) (Wahr et al., 1998).

344 For each monthly solution, the long-term mean of 2003 to 2013 was
345 removed from the monthly spherical harmonic coefficients. Estimates of
346 monthly terrestrial water-storage anomalies were obtained from the residual
347 coefficients using an integration approach described in Wahr et al. (1998). A
348 regional average of the terrestrial water-storage was then computed by defin-
349 ing the mask following the method described in Swenson & Wahr (2002).
350 In addition, we used GLDAS-NOAH estimated total water content (i.e., soil
351 moisture, canopy water, snow and ice) to compute basin scale gain factor
352 as described in Landerer & Swenson (2012); total water content values from
353 NOAH simulated GLDAS were first converted to Stokes’s coefficients and

the two step approach used in filtering GRACE data applied. The results were then reconverted to the spatial domain in the original grid. The original unfiltered GLDAS-derived total water content grid was used as a reference to compute basin scale gain factor as:

$$\varepsilon = \sum_{t_1}^{t_n} (\Delta S_T - k \Delta S_F)^2, \quad (1)$$

where ε is the leakage obtained by finding the root mean difference between the true signal ΔS_T and the filtered signal ΔS_F . The gain factor k , is obtained through a least squares minimization. It is important to note that the scale factor does not match the GRACE-derived water-storage to those of GLDAS rather, it only gives the relative signal attenuation and restores the signal to its “original” form (Landerer & Swenson, 2012). Thus, when working with other gridded datasets (e.g., GLDAS, MODIS and TRMM), one only needs to scale the GRACE signals with the gain factor for consistent comparisons.

3.2.2. Terrestrial water budget

Evapotranspiration estimates using the instantaneous water balance equation in a given basin is expressed as (Brutsaert, 2008, p. 142):

$$ET = P + [(Q_{ri} + Q_{gi}) - (Q_{ro} + Q_{go})] - \frac{dS}{dt}, \quad (2)$$

where P is the area mean rate of precipitation; Q_{ri} is the total surface inflow, Q_{ro} is the total surface outflow, Q_{gi} is the total groundwater inflow, and Q_{go} is the total groundwater outflow rates, all per unit area; and S is the water volume stored per unit area. For the Volta Basin study case, where its area is bounded by natural divides, the groundwater terms can be considered

negligible and the surface inflow is zero (Brutsaert, 2008, p. 142). In such situation, $Q = Q_{ro}$, i.e. the mean net surface runoff rate per unit area from the basin, thus Eq. (2) can be simplified as:

$$ET = P - Q - \frac{dS}{dt}. \quad (3)$$

To obtain monthly values of ET , daily precipitation and discharge measurements must be aggregated to agree with the monthly terrestrial water-storage changes. Since the water balance approach uses station measured net stream flow (hereafter referred to as discharge), it is not able to provide the spatial variation of ET ; however, it is ideal for estimating ET at the basin scale.

Equation (3) can be solved directly for ET as:

$$ET = P - Q - \Delta S, \quad (4)$$

where P presents the monthly values of precipitation, Q stands for discharge, and

$$\Delta S = S(t_2) - S(t_1), \quad (5)$$

indicates water-storage variation between times t_1 and t_2 in which the subscripts 1 and 2 refer to the beginning and the end of the month. For a long period (usually an annual time-scale) ΔS is usually assumed negligible (Xue et al., 2013), i.e., $\Delta S = 0$ assuming a steady state. We will investigate (section 4.2) whether this assumption, i.e. $ET \approx P - Q$, is reasonable at seasonal time scale over the Volta Basin.

Given that the difference between S and δS is a constant value, i.e., mean of the study period, the following equation can be derived from numerical

395 differentiation using the central derivative operator (Ramillien et al., 2006):

$$\Delta S_i = \frac{1}{2} (\delta S_{i+1} - \delta S_{i-1}), \quad (6)$$

396 where ΔS_i is the approximation of water-storage changes during month i .
 397 Equation (6) will be used to provide ΔS in Eq. (4).

398 Another possibility for (3) is based on the standard combined atmosphere-
 399 land water balance equation (Serreze et al., 2006; Landerer et al., 2010)

$$\frac{dS}{dt} = - \left(\frac{\partial W}{\partial t} + \nabla \cdot \mathbf{Q} \right) - Q, \quad (7)$$

400 where $\partial W / \partial t$ represents the change in precipitable water (W) in the at-
 401 mosphere (the water depth of the vapor in the column) and $\nabla \cdot \mathbf{Q}$ is the
 402 divergence of the horizontal water vapor flux \mathbf{Q} integrated from the surface
 403 to the top of the column. Equation (7) will be used to assess the relative
 404 consistence between GRACE-derived water-storage changes (ΔS) and those
 405 estimated using climatological data from ERA-Interim (ΔS^*).

406 3.2.3. Uncertainty

407 Error estimates for remote sensing missions often rely on ground truth
 408 validation (Wahr et al., 2006). For GRACE-derived mass anomalies, the
 409 relative uncertainties were estimated using only GRACE fields as shown by
 410 Wahr et al. (2006). However, GRACE errors can be better estimated us-
 411 ing full covariance matrix (Jensen et al., 2013) and error in the background
 412 model as shown, e.g., by Forootan et al. (2014a). For the background model,
 413 GRACE Atmosphere and Ocean Dealiasing Level 1B (GRACE-AOD1B)
 414 product (Flechtner, 2007) have been used to reduce high frequency non tidal
 415 oceanic and atmospheric mass changes. However, Forootan et al. (2014a)

show that two jumps occur in the atmospheric part of the GRACE-AOD1B products during January-February of the years 2006 and 2010 due to changes of vertical and horizontal resolution in the European Centre for Medium-Range Weather Forecasts operational analysis (ECMWFop).

In fact these jumps impact on GRACE-derived water-storage anomalies inverted from spherical harmonic coefficients and must be corrected for either through updating uncertainty budgets or by applying corrections to estimated trends, amplitudes and phases (Forootan et al., 2014a). These biases were accounted for by modifying monthly GRACE L2 products using an improved model of atmospheric mass variations namely ITG3D-ERA-Interim. This model is based on a modified 3D integration approach (ITG3D) using long-term consistent atmospheric fields from the ERA-Interim (Forootan et al., 2013, 2014a).

The uncertainties in monthly estimates of ET can be computed at 95% confidence level ($\pm\sigma_{ET}ET$) by error propagation through Eq. (4) as suggested by Rodell et al. (2004a):

$$\sigma_{ET} = \frac{\sqrt{\sigma_P^2 P^2 + \sigma_Q^2 Q^2 + \sigma_{\Delta S}^2 \Delta S^2}}{|P - Q - \Delta S|}, \quad (8)$$

where σ_P , σ_Q and $\sigma_{\Delta S}$ are the uncertainties in the monthly precipitation, observed discharge, and GRACE-derived water-storage changes, respectively. Here we assume an error of 10% for precipitation (P) consistent with Thieme et al. (2012), and a conservative value of 10% for the observed discharge (Q). Di Baldassarre & Montanari (2009) pointed out that the uncertainty in discharge data is often considered to be negligible with respect to other approximations affecting hydrological studies. The error for GRACE-derived

439 water-storage anomalies (δS) was estimated by using the calibrated error of
 440 spherical harmonic coefficients propagated, e.g., in Eq. (28) of [Swenson &](#)
 441 [Wahr \(2002\)](#). To account for the month-to-month variations in Eq. (6), the
 442 $\pm\sigma_{\Delta S}\Delta S$ is obtained by multiplying the error in water-storage anomaly by
 443 $\sqrt{2}$.

444 3.2.4. Multi-linear regression analysis (MLRA)

445 Following [Awange et al. \(2011\)](#), multi-linear regression analysis (MLRA)
 446 can be applied to examine the temporal variabilities of the hydrological quan-
 447 tities such as estimated ET . [Rodell et al. \(2011\)](#) pointed out that it is useful
 448 to examine the mean annual cycles, in which the confidence is greater, due
 449 to the uncertainty in the monthly water budget estimates. Hence, for a given
 450 time series, the model used in this work is given by taking into account a
 451 constant (a_0), linear (a_1), annual and semi-annual amplitudes (A_1 and A_2 ,
 452 i.e., occurring once and twice a year, respectively) and phases (ϕ_1 and ϕ_2) as
 453 in [Awange et al. \(2011\)](#):

$$y(t) = a_0 + a_1t + \sum_{k=1}^2 A_k \cos(k\omega t - \phi_k), \quad (9)$$

454 where t is a given time point expressed in years; y is the original input series;
 455 $\omega = 2\pi/T$, where $T = 1$ year in this study; and k represents the rank of
 456 the harmonics ($k = 1$ and $k = 2$ correspond to the annual and semi-annual
 457 components, respectively). The parameters were estimated using a least
 458 squares fitting procedure with their corresponding accuracies. The ET , ΔS ,
 459 and precipitation time series are then analyzed to look for amplitude ratio,
 460 phase lag, and linear trends.

461 3.2.5. Ensemble average (ET_a)

462 Since the ET measurements are scarce over the Volta Basin, an ensemble
 463 average approach can be used to combine the available ET estimates
 464 while considering their uncertainties. A combined ET time series can be cre-
 465 ated based on the six ET products (Modis, VIC, NOAH, MOSAIC, CLM,
 466 GRACE) as:

$$ET_a(t) = \sum_{i=1}^6 w_i(t) ET_i(t), \quad (10)$$

467 where $w_i(t)$ is the time-dependent normalized weight given as

$$w_i = \frac{\frac{1}{\sigma_{ET_i}^2}}{\sum_{j=1}^6 \frac{1}{\sigma_{ET_j}^2}}, \quad (11)$$

468 which reflects the quality of $ET_i(t)$ at time t . The uncertainties for GLDAS
 469 models (VIC, CLM, NOAH and MOSAIC) and MODIS were estimated using
 470 the generalized three-cornered hat method (Gray & Allan, 1974; Premoli &
 471 Tavella, 1993) while TWB-based ET from Eq. (8). This method provides
 472 individual estimation of uncertainties if at least three time series of the same
 473 process are available (Koot et al., 2006).

474 4. Results and Discussions

475 4.1. Evaluation of GRACE-derived water-storage changes

476 Time series of total water-storage changes from February 2003 to Novem-
 477 ber 2012 derived from three different processing centers of CSR, GFZ, and
 478 JPL are shown in Fig. 2(a). Overall, the results presented in Fig. 2(a) show
 479 a good agreement among the three processing centers over the study region.

480 Cross-correlation was carried out between the three time series of water-
 481 storage changes and values of 0.98 between CSR and GFZ, 0.98 between
 482 CSR and JPL, and 0.97 between GFZ and JPL were found. All the three
 483 GRACE solutions show comparable standard deviation signals between 40.44
 484 mm (CSR), 39.65 mm (GFZ) and 41.14 mm (JPL) capturing the range of
 485 variability. The results from CSR, GFZ, and JPL are therefore statistically
 486 identical (comparison of variances at the 95% confidence level) over the Volta
 487 Basin. For the remainder of this study, we utilized only the water-storage
 488 changes estimated from GFZ due to the fact that it had the smallest stan-
 489 dard deviation and also calibrated uncertainties of the spherical harmonic
 490 coefficients were available.

491 **[Figure 2 around here.]**

492 Assessing temporal bias between $P - ET$ and GRACE data might give
 493 in-sights to the biases reported in the reanalysis data. Independently, we
 494 estimated monthly water-storage changes (ΔS^*) for Volta Basin from cli-
 495 matological data ($P - ET$) calculated by using the datasets described in
 496 sub-section 3.1.6 from ERA-Interim and observed discharge data (Q) apply-
 497 ing Eq. (7). Velicogna et al. (2012) stated that there is an unknown bias in
 498 $P - ET$ from reanalysis, which is difficult to estimate. Here, we find a bias of
 499 -25.15 mm/month to close the water budget from February 2003 to November
 500 2012 at Volta Basin, and a RMSE of 41.05 mm/month between the two time
 501 series ($P - ET$ and GRACE). The cross-correlation value associated with
 502 the ΔS^* and GRACE-derived ΔS solutions is 0.51. The standard deviation
 503 of each time series is 39.72 mm/month for GRACE and 35.88 mm/month for

504 ΔS^* with a standard deviation (SD) of the differences of 32.44 mm/month.
 505 The signal-to-noise ratio (SNR) for GRACE and ΔS^* is 1.2 and 1.1, re-
 506 spectively, indicating that further investigation of these products should be
 507 performed over this particular basin.

508 The linear trend, amplitudes, and phases were estimated through a least
 509 squares fitting procedure with their corresponding uncertainties as in Eq. (9),
 510 and are summarized in Table 1. The Volta Basin shows a decrease in ΔS of -
 511 0.00 ± 0.37 mm/year from GRACE and -4.49 ± 0.70 mm/year for ΔS^* , which
 512 is equivalent to -1.85 ± 0.29 km³/yr. The SNR of inter-annual trends for the
 513 water-storage changes are 0.01 mm/year and 6.4 mm/year for GRACE and
 514 ΔS^* , respectively, indicating that GRACE trend is insignificant. Both time
 515 series are characterized by wide variability between dry and wet seasons and
 516 from year to year, which coincides in phase (-0.1 ± 0.2 months) but the ΔS^*
 517 signal has a smaller amplitude (amplitude ratio of 1.7).

518 **[Table 1 around here.]**

519 The TRMM rainfall shows a similar seasonal pattern (Fig. 2(b)) to those
 520 derived from GRACE products. The two time series (TRMM and GRACE)
 521 present cross-correlation value of 0.93 and phase lag of approximately -0.5
 522 ± 0.1 months at the maximum peaks (rainfall lags water-storage changes)
 523 with an amplitude ratio of 1.7. The derived large ratio indicates that the
 524 annual variations of the water-storage within the Volta Basin is dominated by
 525 precipitation. A possible explanation for this phase shift is the evidence of the
 526 basin saturation at 51 mm/month of equivalent water height at the annual
 527 time-scale (e.g., Crowley et al., 2006; Ferreira et al., 2014). Additionally, an

insignificant trend of -0.49 ± 0.60 mm/year that would suggest a decrease in precipitation over the basin during the period under consideration was seen. Paeth et al. (2011) have reported an anomalous wet condition occurred along of the Guinean Coast in July 2007 responsible for 2007 flood in sub-Saharan Africa (cf., Fig. 2(b)). The authors have attributed this to the La Niña event in the Tropical Pacific, anomalous heating in the Tropical Atlantic associated with greater depth of the monsoonal westerlies and enhanced activity of African easterly waves. Also, the available fresh water $P - ET$ (Fig 2(c)) shows a significant decrease in the basin at a rate of -4.10 ± 0.70 mm/year while discharge has a significant increase of 0.39 ± 0.04 mm/year (cf. Table 1).

4.2. Evaluation of global evapotranspiration estimates for Volta Basin

To compare different estimations of ET over the Volta Basin, we computed basin averaged values from GRACE, GLDAS and MODIS data, as well as, an approximation $ET \approx P - Q$ (Fig. 3) that provide seven time series (2 from TWB approach of where one considers GRACE-derived TWS (ET_{TWB}) and the other ignoring it (ET_{P-Q}), 4 from GLDAS-(NOAH, MOSAIC, VIC, CLM), and 1 from MODIS). The error bars in ET_{TWB} were calculated using the Eq. (8) at 95% confidence, for details see sub-section 3.2.3. The results of the comparisons of the GLDAS-simulated, TWB-derived, and MODIS regional ET , as well as $P - Q$ values, show distinct values among them (Fig. 3). The GLDAS solutions (VIC, CLM, NOAH and MOSAIC) are not in agreement with each other, for example, VIC seems to overestimate ET . It is also worth noting that the VIC model seems to have higher amplitudes compared to the other three models. As can be seen from Fig. 3, ET series are quite diverse and makes the decision on which approach provides the best ET esti-

553 mation over the Volta Basin, relative to the ensemble average ET_a even more
 554 difficult. Finally, a combined series ET_a was computed using a weighted av-
 555 erage of ET_{TWB} , ET_{MODIS} , ET_{CLM} , ET_{MOSAIC} , ET_{VIC} and ET_{NOAH} (details
 556 are presented in sub-section 3.2.5).

557 **[Figure 3 around here.]**

558 To infer on the solution that yields the best ET estimates over the Volta
 559 Basin, we provide a concise statistical summary of how well the different
 560 models match each other in terms of correlation coefficient (R), SD, and
 561 root-mean-square-error (RMSE) computed for each dataset with the TWB-
 562 based results is provided here. Thus, the relative performance of the different
 563 models can be inferred from Table 2. The best performing solution must have
 564 the highest correlation coefficient, lowest RMSE, and closest standard devi-
 565 ation relative to the reference model (ET_a). Generally, all the investigated
 566 ET products in Fig. 3 show good correlations with ET_a , with ET_{TWB} being
 567 the lowest (0.82) possibly due to the high uncertainties in ΔS (Fig. 2(a)).
 568 The MODIS solution seems to underestimate ET in the basin with a bias of
 569 -5.30 mm/month, while ET_{TWB} overestimate with a bias of 4.86 mm/month.
 570 [Ruhoff et al. \(2013\)](#) showed that MOD16 algorithm has a tendency to un-
 571 derestimate the average ET at the basin scale for almost all land use and
 572 cover types. [Zeng et al. \(2014\)](#) also reported that MOD16 ET tends to be
 573 underestimated, specially for basins with high ET values.

574 **[Table 2 around here.]**

575 RMSE of 19.39 mm/month was derived when comparing TWB-based
 576 ET to that of ET_a . The corresponding RMSEs for MODIS and GLDAS

577 models (NOAH, CLM, MOSAIC, and VIC) were 6.63 mm/month, 11.77
 578 mm/month, 12.16 mm/month, 18.41 mm/month, and 20.38 mm/month, re-
 579 spectively (e.g., Table 2). Thus, the TWB-based (ET_{TWB}) result is closer
 580 to the reference (ET_a) compared to those of VIC (ET_{VIC}). Among GLDAS
 581 simulations of ET , those derived from NOAH, CLM and MOSAIC seems to
 582 be more accurate than VIC over the Volta Basin. Estimates of VIC were
 583 found to represent a pattern that is not consistent with ET_a estimations. It
 584 should be mentioned here that the RMSE of the TWB-estimated ET values
 585 are in agreement with previous studies (e.g., Rodell et al., 2004a; Ramil-
 586 lien et al., 2006; Cesanelli & Guarracino, 2011; Zeng et al., 2014), i.e., our
 587 GRACE estimations are closer to the ensemble mean.

588 The Taylor diagram (Taylor, 2001) (Fig. 4) presents the results of sta-
 589 tistical comparisons between the ET_a and ET obtained from the four prod-
 590 ucts of GLDAS (VIC, NOAH, MOSAIC and CLM), TWB-based, and that
 591 estimated from MODIS. Among the individual standard deviation of each
 592 time series, only MODIS (28.12 mm/month), NOAH (32.74 mm/month) and
 593 GRACE (32.84 mm/month) were found to represent the range of variability
 594 close to the reference (30.25 mm/month). Additionally, sample compari-
 595 son of variances show that MODIS-estimated ET , NOAH-simulated ET and
 596 TWB-based ET are identical of those derived from ET_a . Xue et al. (2013)
 597 pointed out that the uncertainties in the GLDAS ET products come from
 598 various sources such as meteorological and surface cover data, as well as the
 599 algorithms that are used for its estimations. Further research is necessary
 600 to assess their impact on the simulated ET . However, from this particular
 601 study, by considering the methodology and dataset applied as well as time

span, the NOAH model was found to simulate ET best over Volta Basin compared to the others GLDAS's three models (i.e., CLM, MOSAIC and VIC).

[Figure 4 around here.]

In addition, from our numerical analysis, we the assumption of $\Delta S = 0$ (i.e., assumed steady state) could be questionable over the Volta Basin. Mean annual ΔS is approximately 4% of the corresponding $P - Q$ (Figure 5(a)). However, for semi-arid regions with a pronounced separation between wet and dry seasons (cf. Figure 5(b)), it is reasonable to consider this term in the water balance approach at seasonal time scales, while estimating ET in the basin. From Table 2 and Fig. 4 the improvement of the ET_{TWB} in comparison with ET_{P-Q} . Additionally, the advantage of including GRACE-derived ΔS is that the phase and amplitude of the annual cycle of ET can be ascertained as shown in Rodell et al. (2011). For example, the annual phase and amplitude of ET_{P-Q} are 84.7 mm/month and -5.1 months, ET_{TWB} are 38.6 mm/month and -4.4 months, and ET_a are 45.1 mm/month and -4.6 months, respectively.

[Figure 5 around here.]

It should be mentioned here that the results obtained from the method proposed in this study are based mainly on GRACE-derived water-storage changes, TRMM precipitation data, and in-situ discharge data at Akosombo Dam. This discharge data was regularized over the study period impacting

the water balance over the Volta Basin. Thus, we expect that the TRMM-estimated precipitations (P) are perhaps biased by approximately 11% (underestimation) as shown, e.g., in [Thiemig et al. \(2012\)](#). However, [Rodell et al. \(2011\)](#) concluded that precipitation is not be the most important determinant of bias in modeled ET . Because the modeled ET comes from different data and methods, and they are similar to each other over Volta Basin, it can sufficiently be concluded that they are a good representation of the reality.

5. Conclusion

This study assessed different estimations of evapotranspiration (ET) products based on remote sensing and hydrological model simulations, over the Volta Basin, West Africa, what so far has been elusive due to data scarcity in the region. The proposed approach did not use ground data, which are usually required to validate remotely sensed products, and as such is advantageous where ground data are scarce or not available. The findings could be of use, e.g., to hydrologists, climatologists, and water resources managers in helping them chose the appropriate ET product. However, the method does not allow an estimation of the absolute error of the ET time series and as such, requires that all the products be evaluated and analyzed together. Comparing seven ET estimations to their ensemble mean (ET_a), this study found that remote sensing-based ET estimated by MODIS presents an uncertainty of 3.99 mm/month, while TWB-based ET presents 18.85 mm/month. Among GLDAS-simulated ET , that of NOAH indicated an uncertainty of 7.06 mm/month and the other three models (MOSAIC, CLM and VIC) represented larger errors of 9.97, 12.22 and 15.40 mm/month, respectively.

648 However, only those ET of MODIS, NOAH and GRACE represent similar
649 patterns to that of the computed reference (ET_a). It is worth to mentioned
650 here that the water-storage changes are important as can be seen an im-
651 provement of 45% in terms of RMSE (cf., Table 2), and cannot be neglected
652 while using the water balance approach at a seasonal time scales. Although
653 ET estimated from GRACE has higher RMSE (19.39 mm/month) relative to
654 the reference, it is comparable to the accuracies obtained in previous studies.
655 Further research is needed to improve the estimation of uncertainties and the
656 combination of ET time series.

657 **Acknowledgements**

658 S.A. Andam-Akorful is grateful to Hohai University for his Ph.D. fund-
659 ing and Kwame Nkrumah University of Science and Technology for granting
660 him a study leave. V. G. Ferreira acknowledges the support of grant from
661 National Natural Science Foundation of China (Grant No. 51208311). We
662 are grateful to Dr. Emmanuel Obeng Bekoe of Water Research Institute,
663 Ghana, for providing discharge data of the Volta Basin. We also thank the
664 GRACE mission satellite team and the CSR, JPL and GFZ for providing
665 the monthly gravity fields. The GLDAS data used in this study were ac-
666 quired as part of the mission of NASA’s Earth Science Division and were
667 archived and distributed by the Goddard Earth Sciences (GES) Data and
668 Information Services Center (DISC). The precipitation product used in this
669 study was from TRMM. We thank Prof. Radan Huth (Editor in Chief) and
670 two anonymous reviewers for their constructive comments that helped us to
671 improve the paper.

672 **References**

- 673 Adeyewa, Z. D., & Nakamura, K. (2003). Validation of TRMM radar rainfall
674 data over major climatic regions in Africa. *Journal of Applied Meteorol-*
675 *ogy*, 42, 331–347. doi:[10.1175/1520-0450\(2003\)042<0331:VOTRRD>2.0.](https://doi.org/10.1175/1520-0450(2003)042<0331:VOTRRD>2.0.CO;2)
676 [CO;2](https://doi.org/10.1175/1520-0450(2003)042<0331:VOTRRD>2.0.CO;2).
- 677 Adjei, K. A., Ren, L., & Appiah-Adjei, E. K. (2012). Validation of TRMM
678 data in the Black Volta Basin of Ghana. *Journal of Hydrologic Engineer-*
679 *ing*, 17, 647–654. doi:[10.1061/\(ASCE\)HE.1943-5584.0000487](https://doi.org/10.1061/(ASCE)HE.1943-5584.0000487).
- 680 Allen, R. G., Tasumi, M., Morse, A., Trezza, R., Wright, J. L., Bastiaanssen,
681 W., Kramber, W., Lorite, I., & Robison, C. W. (2007). Satellite-based en-
682 ergy balance for mapping evapotranspiration with internalized calibration
683 (metric) - applications. *Journal of Irrigation and Drainage Engineering*,
684 133, 395–406. doi:[10.1061/\(ASCE\)0733-9437\(2007\)133:4\(395\)](https://doi.org/10.1061/(ASCE)0733-9437(2007)133:4(395)).
- 685 Alton, P., Fisher, R., Los, S., & Williams, M. (2009). Simulations of
686 global evapotranspiration using semiempirical and mechanistic schemes of
687 plant hydrology. *Global Biogeochemical Cycles*, 23, GB4023. doi:[10.1029/](https://doi.org/10.1029/2009GB003540)
688 [2009GB003540](https://doi.org/10.1029/2009GB003540).
- 689 Andreini, M., van de Giesen, N., van Edig, A., Fosu, M., & Andah, W.
690 (2000). *Volta Basin Water Balance*. Discussion Papers on Development
691 Policy 21 Zentrum für Entwicklungsforschung Bonn. URL: [http://www.](http://www.zef.de/fileadmin/webfiles/downloads/zef_dp/zef-dp21-00.pdf)
692 [zef.de/fileadmin/webfiles/downloads/zef_dp/zef-dp21-00.pdf](http://www.zef.de/fileadmin/webfiles/downloads/zef_dp/zef-dp21-00.pdf).
- 693 Awange, J., Fleming, K., Kuhn, M., Featherstone, W., Heck, B., & Anjas-
694 mara, I. (2011). On the suitability of the $4^{\circ} \times 4^{\circ}$ GRACE mascon solutions

- 695 for remote sensing Australian hydrology. *Remote Sensing of Environment*,
696 115, 864875. doi:[10.1016/j.rse.2010.11.014](https://doi.org/10.1016/j.rse.2010.11.014).
- 697 Bastiaanssen, W., Pelgrum, H., Wang, J., Ma, Y., Moreno, J., Roerink, G., &
698 van der Wal, T. (1998). A remote sensing surface energy balance algorithm
699 for land (SEBAL).: Part 2: Validation. *Journal of Hydrology*, 212–213,
700 213–229. doi:[10.1016/S0022-1694\(98\)00254-6](https://doi.org/10.1016/S0022-1694(98)00254-6).
- 701 Bettadpur, S. (2012a). *Gravity Recovery and Climate Experiment: Level-2*
702 *Gravity Field Product User Handbook*. Technical Report Center for Space
703 Research, The University of Texas at Austin Austin, Texas.
- 704 Bettadpur, S. (2012b). *Gravity Recovery and Climate Experiment: Product*
705 *Specification Document*. Technical Report Center for Space Research, The
706 University of Texas at Austin Austin, Texas.
- 707 Boronina, A., & Ramillien, G. (2008). Application of AVHRR imagery and
708 GRACE measurements for calculation of actual evapotranspiration over
709 the Quaternary aquifer (Lake Chad basin) and validation of groundwa-
710 ter models. *Journal of Hydrology*, 348, 98–109. doi:[10.1016/j.jhydrol.](https://doi.org/10.1016/j.jhydrol.2007.09.061)
711 [2007.09.061](https://doi.org/10.1016/j.jhydrol.2007.09.061).
- 712 Boy, J.-P., Hinderer, J., & Linage, C. (2012). Retrieval of large-scale hydro-
713 logical signals in Africa from GRACE time-variable gravity fields. *Pure and*
714 *Applied Geophysics*, 169, 1373–1390. doi:[10.1007/s00024-011-0416-x](https://doi.org/10.1007/s00024-011-0416-x).
- 715 Bruinsma, S., Lemoine, J.-M., Biancale, R., & Valès, N. (2010).
716 CNES/GRGS 10-day gravity field models (release 2) and their evaluation.

- 717 *Advances in Space Research*, 45, 587–601. doi:[10.1016/j.asr.2009.10.](https://doi.org/10.1016/j.asr.2009.10.012)
718 [012](https://doi.org/10.1016/j.asr.2009.10.012).
- 719 Brutsaert, W. (2008). *Hydrology: An Introduction*. (illustrate ed.). Cam-
720 bridge University Press.
- 721 Cazenave, A., & Chen, J. (2010). Time-variable gravity from space and
722 present-day mass redistribution in the Earth system. *Earth and Planetary*
723 *Science Letters*, 298, 263–274. doi:[10.1016/j.epsl.2010.07.035](https://doi.org/10.1016/j.epsl.2010.07.035).
- 724 Cesanelli, A., & Guarracino, L. (2011). Estimation of regional evapotran-
725 spiration in the extended Salado Basin (Argentina) from satellite grav-
726 ity measurements. *Hydrogeology Journal*, 19, 629–639. doi:[10.1007/](https://doi.org/10.1007/s10040-011-0708-3)
727 [s10040-011-0708-3](https://doi.org/10.1007/s10040-011-0708-3).
- 728 Chen, J. L., Wilson, C. R., Tapley, B. D., Longuevergne, L., Yang, Z. L., &
729 Scanlon, B. R. (2010). Recent La Plata basin drought conditions observed
730 by satellite gravimetry. *Journal of Geophysical Research*, 115, D22108.
731 doi:[10.1029/2010JD014689](https://doi.org/10.1029/2010JD014689).
- 732 Cheng, M., & Tapley, B. D. (2004). Variations in the Earth’s oblateness
733 during the past 28 years. *J. Geophys. Res.*, 109, B09402. doi:[10.1029/](https://doi.org/10.1029/2004JB003028)
734 [2004JB003028](https://doi.org/10.1029/2004JB003028).
- 735 Cheng, M., Tapley, B. D., & Ries, J. C. (2013). Deceleration in the earth’s
736 oblateness. *Journal of Geophysical Research: Solid Earth*, 118, 740–747.
737 doi:[10.1002/jgrb.50058](https://doi.org/10.1002/jgrb.50058).
- 738 Cleugh, H. A., Leuning, R., Mu, Q., & Running, S. W. (2007). Regional

739 evaporation estimates from flux tower and MODIS satellite data. *Remote*
740 *Sensing of Environment*, 106, 285–304. doi:[10.1016/j.rse.2006.07.007](https://doi.org/10.1016/j.rse.2006.07.007).

741 Compaoré, H., Hendrickx, J. M. H., Hong, S.-h., Friesen, J., van de Giesen,
742 N. C., Rodgers, C., Szarzynski, J., & Vlek, P. L. G. (2008). Evaporation
743 mapping at two scales using optical imagery in the White Volta Basin,
744 Upper East Ghana. *Physics and Chemistry of the Earth, Parts A/B/C*,
745 33, 127–140. doi:[10.1016/j.pce.2007.04.021](https://doi.org/10.1016/j.pce.2007.04.021). Hydrological Assessment
746 and Integrated Water Resources Management with Special Focus on De-
747 veloping Countries.

748 Cox, C. M., & Chao, B. F. (2002). Detection of a large-scale mass redis-
749 tribution in the terrestrial system since 1998. *Science*, 297, 831–833.
750 doi:[10.1126/science.1072188](https://doi.org/10.1126/science.1072188).

751 Crowley, J. W., Mitrovica, J. X., Bailey, R. C., Tamisiea, M. E., &
752 Davis, J. L. (2006). Land water storage within the congo basin in-
753 ferred from grace satellite gravity data. *Geophysical Research Letters*,
754 33, n/a–n/a. URL: <http://dx.doi.org/10.1029/2006GL027070>. doi:[10.](https://doi.org/10.1029/2006GL027070)
755 [1029/2006GL027070](https://doi.org/10.1029/2006GL027070).

756 Dai, Y., Zeng, X., Dickinson, R. E., Baker, I., Bonan, G. B., Bosilovich,
757 M. G., Denning, A. S., Dirmeyer, P. A., Houser, P. R., Niu, G., & et al.
758 (2003). The common land model. *Bulletin of the American Meteorological*
759 *Society*, 84, 10131023. doi:[10.1175/BAMS-84-8-1013](https://doi.org/10.1175/BAMS-84-8-1013).

760 Dee, D. P., Uppala, S. M., Simmons, A. J., Berrisford, P., Poli, P., Kobayashi,
761 S., Andrae, U., Balmaseda, M. A., Balsamo, G., Bauer, P., & et al. (2011).

- 762 The ERA-Interim reanalysis: configuration and performance of the data
763 assimilation system. *Quarterly Journal of the Royal Meteorological Society*,
764 *137*, 553597. doi:[10.1002/qj.828](https://doi.org/10.1002/qj.828).
- 765 Di Baldassarre, G., & Montanari, A. (2009). Uncertainty in river discharge
766 observations: a quantitative analysis. *Hydrology and Earth System Sci-*
767 *ences*, *13*, 913–921. doi:[10.5194/hess-13-913-2009](https://doi.org/10.5194/hess-13-913-2009).
- 768 Duan, X. J., Guo, J. Y., Shum, C. K., & Wal, W. (2009). On the postprocess-
769 ing removal of correlated errors in GRACE temporal gravity field solutions.
770 *Journal of Geodesy*, *83*, 1095–1106. doi:[10.1007/s00190-009-0327-0](https://doi.org/10.1007/s00190-009-0327-0).
- 771 Ek, M. B., Mitchell, K. E., Lin, Y., Rogers, E., Grunmann, P., Koren, V.,
772 Gayno, G., & Tarpley, J. D. (2003). Implementation of Noah land sur-
773 face model advances in the National Centers for Environmental Prediction
774 operational mesoscale Eta model. *Journal of Geophysical Research*, *108*,
775 8851. doi:[10.1029/2002JD003296](https://doi.org/10.1029/2002JD003296).
- 776 Estes, L. D., Chaney, N., Herrera-Estrada, J., Caylor, K. K., Sheffield, J.,
777 & Wood, E. F. (2013). Spatial Trends in Evapotranspiration Components
778 over Africa between 1979 and 2012 and Their Relative Influence on Crop
779 Water Use. *AGU Fall Meeting Abstracts*, (p. A3).
- 780 Ferreira, V. G., Andam-Akorful, S. A., He, X.-f., & Xiao, R.-y. (2014). Esti-
781 mating water storage changes and sink terms in Volta Basin from satellite
782 missions. *Water Science and Engineering*, *7*, 5–16. doi:[10.3882/j.issn.](https://doi.org/10.3882/j.issn.1674-2370.2014.01.002)
783 [1674-2370.2014.01.002](https://doi.org/10.3882/j.issn.1674-2370.2014.01.002).

- 784 Fisher, J. B., Whittaker, R. J., & Malhi, Y. (2011). Et come home: potential
785 evapotranspiration in geographical ecology. *Global Ecology and Biogeogra-*
786 *phy*, 20, 1–18. doi:[10.1111/j.1466-8238.2010.00578.x](https://doi.org/10.1111/j.1466-8238.2010.00578.x).
- 787 Flechtner, F. (2007). AOD1B product description document, version 3.1,
788 GRACE. URL: <http://isdc.gfz-potsdam.de/grace> project Document
789 JPL.
- 790 Fleming, K., & Awange, J. L. (2013). Comparing the version 7 TRMM 3B43
791 monthly precipitation product with the TRMM 3B43 version 6/6A and
792 Bureau of Meteorology datasets for Australia. *Australian Meteorological*
793 *and Oceanographic Journal*, 63, 421–426. URL: [http://www.bom.gov.au/](http://www.bom.gov.au/amm/docs/2013/fleming.pdf)
794 [amm/docs/2013/fleming.pdf](http://www.bom.gov.au/amm/docs/2013/fleming.pdf).
- 795 Forootan, E., Didova, O., Kusche, J., & Löcher, A. (2013). Comparisons
796 of atmospheric data and reduction methods for the analysis of satellite
797 gravimetry observations. *Journal of Geophysical Research: Solid Earth*,
798 118, 2382–2396. doi:[10.1002/jgrb.50160](https://doi.org/10.1002/jgrb.50160).
- 799 Forootan, E., Didova, O., Schumacher, M., Kusche, J., & Elsaka, B. (2014a).
800 Comparisons of atmospheric mass variations derived from ECMWF re-
801 analysis and operational fields, over 2003–2011. *Journal of Geodesy*, 88,
802 503–514. doi:[10.1007/s00190-014-0696-x](https://doi.org/10.1007/s00190-014-0696-x).
- 803 Forootan, E., Kusche, J., Loth, I., Schuh, W.-D., Eicker, A., Awange, J.,
804 Longuevergne, L., Diekkrüger, B., Schmidt, M., & Shum, C. (2014b).
805 Multivariate prediction of total water storage anomalies over west africa

806 from multi-satellite data. *Surveys in Geophysics*, 35, 913 – 940. doi:
807 [10.1007/s10712-014-9292-0](https://doi.org/10.1007/s10712-014-9292-0).

808 van de Giesen, N., Liebe, J., & Jung, G. (2010). Adapting to climate change
809 in the Volta Basin, West Africa. *Current Science*, 98, 1033 – 1037.

810 Gray, J., & Allan, D. (1974). A method for estimating the frequency stabil-
811 ity of an individual oscillator. In *28th Annual Symposium on Frequency*
812 *Control* (pp. 243–246). IEEE. doi:[10.1109/FREQ.1974.200027](https://doi.org/10.1109/FREQ.1974.200027).

813 Grippa, M., Kergoat, L., Frappart, F., Araud, Q., Boone, A., de Rosnay,
814 P., Lemoine, J.-M., Gascoin, S., Balsamo, G., Ottlé, C., Decharme, B.,
815 Saux-Picart, S., & Ramillien, G. (2011). Land water storage variability
816 over West Africa estimated by Gravity Recovery and Climate Experiment
817 (GRACE) and land surface models. *Water Resources Research*, 47, n/a–
818 n/a. doi:[10.1029/2009WR008856](https://doi.org/10.1029/2009WR008856).

819 Gyau-Boakye, P., & Tumbulto, J. (2000). The Volta Lake and declining rain-
820 fall and streamflows in the Volta River Basin. *Environment, Development*
821 *and Sustainability*, 2, 1–11. doi:[10.1023/A:1010020328225](https://doi.org/10.1023/A:1010020328225).

822 Hafeez, M., Andreini, M., Liebe, J., Friesen, J., Marx, A., & van de Giesen,
823 N. (2007). Hydrological parameterization through remote sensing in Volta
824 Basin, West Africa. *International Journal of River Basin Management*,
825 5, 49–56. doi:[10.1080/15715124.2007.9635305](https://doi.org/10.1080/15715124.2007.9635305).

826 Hendrickx, J. M. H., Hong, S.-h., Friesen, J., Compaore, H., van de Giesen,
827 N. C., Rodgers, C., & Vlek, P. L. G. (2006). Mapping energy balance
828 fluxes and root zone soil moisture in the White Volta Basin using optical

829 imagery. In W. R. Watkins, & D. Clement (Eds.), *Targets and Backgrounds*
 830 *XII: Characterization and Representation* (p. 62390Q). doi:[10.1117/12.](https://doi.org/10.1117/12.665235)
 831 [665235](https://doi.org/10.1117/12.665235).

832 Hinderer, J., Pfeffer, J., Boucher, M., Nahmani, S., Linage, C., Boy, J.-P.,
 833 Genthon, P., Seguis, L., Favreau, G., Bock, O., & Descloitres, M. (2012).
 834 Land water storage changes from ground and space geodesy: First results
 835 from the GHYRAF (Gravity and Hydrology in Africa) Experiment. *Pure*
 836 *and Applied Geophysics*, 169, 1391–1410. URL: [http://dx.doi.org/10.](http://dx.doi.org/10.1007/s00024-011-0417-9)
 837 [1007/s00024-011-0417-9](http://dx.doi.org/10.1007/s00024-011-0417-9). doi:[10.1007/s00024-011-0417-9](https://doi.org/10.1007/s00024-011-0417-9).

838 Huffman, G. J., Bolvin, D. T., Nelkin, E. J., Wolff, D. B., Adler, R. F.,
 839 Gu, G., Hong, Y., Bowman, K. P., & Stocker, E. F. (2007). The
 840 TRMM multisatellite precipitation analysis (TMPA): Quasi-global, mul-
 841 tiyear, combined-sensor precipitation estimates at fine scales. *Journal of*
 842 *Hydrometeorology*, 8, 38–55. doi:[10.1175/JHM560.1](https://doi.org/10.1175/JHM560.1).

843 Jensen, L., Rietbroek, R., & Kusche, J. (2013). Land water contribution
 844 to sea level from GRACE and Jason-1 measurements. *Journal of Geo-*
 845 *physical Research: Oceans*, 118, 212–226. URL: [http://dx.doi.org/10.](http://dx.doi.org/10.1002/jgrc.20058)
 846 [1002/jgrc.20058](http://dx.doi.org/10.1002/jgrc.20058). doi:[10.1002/jgrc.20058](https://doi.org/10.1002/jgrc.20058).

847 Jung, G., & Kunstmann, H. (2007). High-resolution regional climate model-
 848 ing for the Volta region of West Africa. *Journal of Geophysical Research:*
 849 *Atmospheres*, 112, n/a–n/a. doi:[10.1029/2006JD007951](https://doi.org/10.1029/2006JD007951).

850 Jung, M., Reichstein, M., Ciais, P., Seneviratne, S. I., Sheffield, J., Goulden,
 851 M. L., Bonan, G., Cescatti, A., Chen, J., de Jeu, R., & et al. (2010).

- 852 Recent decline in the global land evapotranspiration trend due to limited
853 moisture supply. *Nature*, 467, 951–954.
- 854 Kasei, R., Diekkrüger, B., & Leemhuis, C. (2009). Drought frequency in
855 the Volta Basin of West Africa. *Sustainability Science*, 5, 89–97. doi:[10.1007/s11625-009-0101-5](https://doi.org/10.1007/s11625-009-0101-5).
- 856
- 857 Klees, R., Liu, X., Wittwer, T., Gunter, B. C., Revtova, E. A., Tenzer, R.,
858 Ditmar, P., Winsemius, H. C., & Savenije, H. H. G. (2008). A comparison
859 of global and regional GRACE models for land hydrology. *Surveys in*
860 *Geophysics*, 29, 335–359. doi:[10.1007/s10712-008-9049-8](https://doi.org/10.1007/s10712-008-9049-8).
- 861 Komatsu, H., Kume, T., & Otsuki, K. (2008). The effect of converting
862 a native broad-leaved forest to a coniferous plantation forest on annual
863 water yield: A paired-catchment study in northern Japan. *Forest Ecology*
864 *and Management*, 255, 880–886. doi:[10.1016/j.foreco.2007.10.010](https://doi.org/10.1016/j.foreco.2007.10.010).
- 865 Koot, L., Viron, O. D., & Dehant, V. (2006). Atmospheric angular mo-
866 mentum time-series: Characterization of their internal noise and creation
867 of a combined series. *Journal of Geodesy*, 79, 663674. doi:[10.1007/s00190-005-0019-3](https://doi.org/10.1007/s00190-005-0019-3).
- 868
- 869 Koster, R. D., & Suarez, M. J. (1996). Energy and water balance calculations
870 in the mosaic lsm. In M. J. Suarez (Ed.), *Technical Report Series on Global*
871 *Modeling and Data Assimilation* (p. 9). volume 9.
- 872 Kousari, M. R., & Ahani, H. (2012). An investigation on reference crop
873 evapotranspiration trend from 1975 to 2005 in Iran. *International Journal*
874 *of Climatology*, 32, 2387–2402. doi:[10.1002/joc.3404](https://doi.org/10.1002/joc.3404).

- 875 Kunstmann, H., & Jung, G. (2007). Influence of soilmoisture and land use
876 change on precipitation in the Volta Basin of West Africa. *International*
877 *Journal of River Basin Management*, 5, 9–16. doi:[10.1080/15715124.](https://doi.org/10.1080/15715124.2007.9635301)
878 [2007.9635301](https://doi.org/10.1080/15715124.2007.9635301).
- 879 Landerer, F. W., Dickey, J. O., & Güntner, A. (2010). Terrestrial water
880 budget of the Eurasian Pan-Arctic from GRACE satellite measurements
881 during 2003–2009. *Journal of Geophysical Research*, 115, D23115. doi:[10.](https://doi.org/10.1029/2010JD014584)
882 [1029/2010JD014584](https://doi.org/10.1029/2010JD014584).
- 883 Landerer, F. W., & Swenson, S. C. (2012). Accuracy of scaled GRACE
884 terrestrial water storage estimates. *Water Resources Research*, 48, 1–11.
885 doi:[10.1029/2011WR011453](https://doi.org/10.1029/2011WR011453).
- 886 Lebel, T., Delclaux, F., Le Barb, L., & Polcher, J. (2000). From GCM
887 scales to hydrological scales: rainfall variability in West Africa. *Stochastic*
888 *Environmental Research and Risk Assessment*, 14, 275–295. doi:[10.1007/](https://doi.org/10.1007/s004770000050)
889 [s004770000050](https://doi.org/10.1007/s004770000050).
- 890 Leemhuis, C., Jung, G., Kasei, R., & Liebe, J. (2009). The Volta Basin water
891 allocation system: assessing the impact of small-scale reservoir develop-
892 ment on the water resources of the Volta Basin, West Africa. *Advances in*
893 *Geosciences*, 21, 57–62. doi:[10.5194/adgeo-21-57-2009](https://doi.org/10.5194/adgeo-21-57-2009).
- 894 Liang, X., Lettenmaier, D. P., Wood, E. F., & Burges, S. J. (1994). A simple
895 hydrologically based model of land surface water and energy fluxes for
896 general circulation models. *Journal of Geophysical Research*, 99, 14415.
897 doi:[10.1029/94JD00483](https://doi.org/10.1029/94JD00483).

- 898 Long, D., Longuevergne, L., & Scanlon, B. R. (2014). Uncertainty in
899 evapotranspiration from land surface modeling, remote sensing, and
900 GRACE satellites. *Water Resources Research*, *50*, 1131–1151. doi:[10.1002/2013WR014581](https://doi.org/10.1002/2013WR014581).
901
- 902 Mitchell, K. E., Lohmann, D., Houser, P. R., Wood, E. F., Schaake, J. C.,
903 Robock, A., Cosgrove, B. A., Sheffield, J., Duan, Q., Luo, L., Higgins,
904 R. W., Pinker, R. T., Tarpley, J. D., Lettenmaier, D. P., Marshall, C. H.,
905 Entin, J. K., Pan, M., Shi, W., Koren, V., Meng, J., Ramsay, B. H., &
906 Bailey, A. A. (2004). The multi-institution north american land data assim-
907 ilation system (nldas): Utilizing multiple gcip products and partners in a
908 continental distributed hydrological modeling system. *Journal of Geophysical
909 Research: Atmospheres*, *109*, n/a–n/a. doi:[10.1029/2003JD003823](https://doi.org/10.1029/2003JD003823).
- 910 Moiwo, J. P., Yang, Y., Yan, N., & Wu, B. (2011). Comparison of evapotran-
911 spiration estimated by ETWatch with that derived from combined GRACE
912 and measured precipitation data in Hai River Basin, North China. *Hy-
913 drological Sciences Journal*, *56*, 249–267. doi:[10.1080/02626667.2011.553617](https://doi.org/10.1080/02626667.2011.553617).
914
- 915 Monteith, J. (1965). Evaporation and environment. *Symp. Soc. Exp. Biol*,
916 (pp. 19:205–234).
- 917 Mu, Q., Heinsch, F. A., Zhao, M., & Running, S. W. (2007). Devel-
918 opment of a global evapotranspiration algorithm based on MODIS and
919 global meteorology data. *Remote Sensing of Environment*, *111*, 519–536.
920 doi:[10.1016/j.rse.2007.04.015](https://doi.org/10.1016/j.rse.2007.04.015).

- 921 Mu, Q., Zhao, M., Kimball, J. S., McDowell, N. G., & Running, S. W.
 922 (2013). A remotely sensed global terrestrial drought severity index. *Bul-*
 923 *letin of the American Meteorological Society*, 94, 83–98. doi:[10.1175/
 924 BAMS-D-11-00213.1](https://doi.org/10.1175/BAMS-D-11-00213.1).
- 925 Mu, Q., Zhao, M., & Running, S. W. (2011). Improvements to a MODIS
 926 global terrestrial evapotranspiration algorithm. *Remote Sensing of Envi-*
 927 *ronment*, 115, 1781–1800. doi:[10.1016/j.rse.2011.02.019](https://doi.org/10.1016/j.rse.2011.02.019).
- 928 Neumann, R., Jung, G., Laux, P., & Kunstmann, H. (2007). Climate trends
 929 of temperature, precipitation and river discharge in the Volta Basin of
 930 West Africa. *International Journal of River Basin Management*, 5, 17–
 931 30. doi:[10.1080/15715124.2007.9635302](https://doi.org/10.1080/15715124.2007.9635302).
- 932 Nicholson, S. E. (2013). The West African Sahel: A review of recent studies
 933 on the rainfall regime and its interannual variability. *ISRN Meteorology*,
 934 2013, 1–32. doi:[10.1155/2013/453521](https://doi.org/10.1155/2013/453521).
- 935 Nicholson, S. E., Some, B., McCollum, J., Nelkin, E., Klotter, D., Berte,
 936 Y., Diallo, B. M., Gaye, I., Kpabeba, G., Ndiaye, O., & et al. (2003).
 937 Validation of TRMM and other rainfall estimates with a high-density
 938 gauge dataset for West Africa. Part II: Validation of TRMM rainfall
 939 products. *Journal of Applied Meteorology*, 42, 1355–1368. doi:[10.1175/
 940 1520-0450\(2003\)042<1355:VOTAOR>2.0.CO;2](https://doi.org/10.1175/1520-0450(2003)042<1355:VOTAOR>2.0.CO;2).
- 941 Oguntunde, P. (2004). *Evapotranspiration and complimentarity relations*
 942 *in the water balance of the Volta Basin: Field measurements and GIS-*

- 943 *based regional estimates*. Number 22 in Ecology and Development Series.
944 Göttingen, Germany: Cuvillier Verlag.
- 945 Oguntunde, P. G., Friesen, J., van de Giesen, N., & Savenije, H. H. (2006).
946 Hydroclimatology of the Volta River Basin in West Africa: Trends and
947 variability from 1901 to 2002. *Physics and Chemistry of the Earth, Parts*
948 *A/B/C*, *31*, 1180–1188. doi:[10.1016/j.pce.2006.02.062](https://doi.org/10.1016/j.pce.2006.02.062). Time Series
949 Analysis in Hydrology.
- 950 Opoku-Duah, S., Donoghue, D., & Burt, T. P. (2008). Intercomparison of
951 evapotranspiration over the Savannah Volta Basin in West Africa using
952 remote sensing data. *Sensors*, *8*, 2736–2761. doi:[10.3390/s8042736](https://doi.org/10.3390/s8042736).
- 953 Owusu, K., Waylen, P., & Qiu, Y. (2008). Changing rainfall inputs in the
954 volta basin: implications for water sharing in Ghana. *GeoJournal*, *71*,
955 201–210. doi:[10.1007/s10708-008-9156-6](https://doi.org/10.1007/s10708-008-9156-6).
- 956 Oyebande, L., & Odunuga, S. (2010). Climate change impact on water
957 resources at the transboundary level in West Africa: The cases of the
958 Senegal, Niger and Volta Basins. *Open Hydrology Journal*, *4*, 163–172.
959 doi:[10.2174/1874378101004010163](https://doi.org/10.2174/1874378101004010163).
- 960 Paeth, H., Fink, A. H., Pohle, S., Keis, F., Mächel, H., & Samimi, C. (2011).
961 Meteorological characteristics and potential causes of the 2007 flood in
962 sub-Saharan Africa. *International Journal of Climatology*, *31*, 1908–1926.
963 doi:[10.1002/joc.2199](https://doi.org/10.1002/joc.2199).
- 964 Pôças, I., Cunha, M., Pereira, L. S., & Allen, R. G. (2013). Using remote
965 sensing energy balance and evapotranspiration to characterize montane

966 landscape vegetation with focus on grass and pasture lands. *International*
 967 *Journal of Applied Earth Observation and Geoinformation*, *21*, 159–172.
 968 doi:<http://dx.doi.org/10.1016/j.jag.2012.08.017>.

969 Premoli, A., & Tavella, P. (1993). A revisited three-cornered hat method for
 970 estimating frequency standard instability. *IEEE Transactions on Instru-*
 971 *mentation and Measurement*, *42*, 713. doi:[10.1109/19.206671](https://doi.org/10.1109/19.206671).

972 Ramillien, G., Frappart, F., Güntner, A., Ngo-Duc, T., Cazenave, A., &
 973 Laval, K. (2006). Time variations of the regional evapotranspiration
 974 rate from Gravity Recovery and Climate Experiment (GRACE) satel-
 975 lite gravimetry. *Water Resources Research*, *42*, W10403. doi:[10.1029/](https://doi.org/10.1029/2005WR004331)
 976 [2005WR004331](https://doi.org/10.1029/2005WR004331).

977 Rodell, M., Famiglietti, J. S., Chen, J., Seneviratne, S. I., Viterbo, P., Holl,
 978 S., & Wilson, C. R. (2004a). Basin scale estimates of evapotranspiration
 979 using GRACE and other observations. *Geophysical Research Letters*, *31*,
 980 L20504. doi:[10.1029/2004GL020873](https://doi.org/10.1029/2004GL020873).

981 Rodell, M., Houser, P. R., Jambor, U., Gottschalck, J., Mitchell, K., Meng,
 982 C.-J., Arsenault, K., Cosgrove, B., Radakovich, J., Bosilovich, M., & et al.
 983 (2004b). The global land data assimilation system. *Bulletin of the Amer-*
 984 *ican Meteorological Society*, *85*, 381–394. doi:[10.1175/BAMS-85-3-381](https://doi.org/10.1175/BAMS-85-3-381).

985 Rodell, M., McWilliams, E. B., Famiglietti, J. S., Beaudoin, H. K., &
 986 Nigro, J. (2011). Estimating evapotranspiration using an observation
 987 based terrestrial water budget. *Hydrological Processes*, *25*, 4082–4092.
 988 doi:[10.1002/hyp.8369](https://doi.org/10.1002/hyp.8369).

- 989 Ruhoff, A. L., Paz, A. R., Aragao, L. E. O. C., Mu, Q., Malhi, Y., Col-
 990 lischonn, W., Rocha, H. R., & Running, S. W. (2013). Assessment of
 991 the MODIS global evapotranspiration algorithm using eddy covariance
 992 measurements and hydrological modelling in the Rio Grande basin. *Hy-*
 993 *drological Sciences Journal*, 58, 1658–1676. doi:[10.1080/02626667.2013.](https://doi.org/10.1080/02626667.2013.837578)
 994 [837578](https://doi.org/10.1080/02626667.2013.837578).
- 995 Sahoo, A. K., Pan, M., Troy, T. J., Vinukollu, R. K., Sheffield, J., & Wood,
 996 E. F. (2011). Reconciling the global terrestrial water budget using satellite
 997 remote sensing. *Remote Sensing of Environment*, 115, 1850–1865. doi:[10.](https://doi.org/10.1016/j.rse.2011.03.009)
 998 [1016/j.rse.2011.03.009](https://doi.org/10.1016/j.rse.2011.03.009).
- 999 Samimi, C., Fink, A. H., & Paeth, H. (2012). The 2007 flood in
 1000 the Sahel: causes, characteristics and its presentation in the me-
 1001 dia and FEWS NET. *Natural Hazards and Earth System Science*,
 1002 12, 313–325. URL: [http://www.nat-hazards-earth-syst-sci.net/12/](http://www.nat-hazards-earth-syst-sci.net/12/313/2012/)
 1003 [313/2012/](http://www.nat-hazards-earth-syst-sci.net/12/313/2012/). doi:[10.5194/nhess-12-313-2012](https://doi.org/10.5194/nhess-12-313-2012).
- 1004 Santos, C., Lorite, I., Tasumi, M., Allen, R., & Fereres, E. (2008). Inte-
 1005 grating satellite-based evapotranspiration with simulation models for irri-
 1006 gation management at the scheme level. *Irrigation Science*, 26, 277–288.
 1007 doi:[10.1007/s00271-007-0093-9](https://doi.org/10.1007/s00271-007-0093-9).
- 1008 Schüttemeyer, D., Schillings, C., Moene, A. F., & de Bruin, H. A. R. (2007).
 1009 Satellite-based actual evapotranspiration over drying semiarid terrain in
 1010 West Africa. *Journal of Applied Meteorology and Climatology*, 46, 97–
 1011 111. doi:[10.1175/JAM2444.1](https://doi.org/10.1175/JAM2444.1).

- 1012 Serreze, M. C., Barrett, A. P., Slater, A. G., Woodgate, R. A., Aagaard, K.,
 1013 Lammers, R. B., Steele, M., Moritz, R., Meredith, M., & Lee, C. M. (2006).
 1014 The large-scale freshwater cycle of the Arctic. *Journal of Geophysical*
 1015 *Research*, *111*, C11010. doi:[10.1029/2005JC003424](https://doi.org/10.1029/2005JC003424).
- 1016 Shahin, M. (2002). Hydrology of selected intermediate and small river
 1017 basins. In *Hydrology and Water Resources of Africa* (pp. 377–425).
 1018 Springer Netherlands volume 41 of *Water Science and Technology Library*.
 1019 doi:[10.1007/0-306-48065-4_9](https://doi.org/10.1007/0-306-48065-4_9).
- 1020 Su, Z. (2002). The surface energy balance system (SEBS) for estimation of
 1021 turbulent heat fluxes SEBS - the surface energy balance. *Hydrology and*
 1022 *Earth System Sciences*, *6*, 85–99. doi:[10.5194/hess-6-85-2002](https://doi.org/10.5194/hess-6-85-2002).
- 1023 Sultan, B., Baron, C., Dingkuhn, M., Sarr, B., & Janicot, S. (2005). Agricul-
 1024 tural impacts of large-scale variability of the West African monsoon. *Agricul-*
 1025 *cultural and Forest Meteorology*, *128*, 93–110. doi:[10.1016/j.agrformet.](https://doi.org/10.1016/j.agrformet.2004.08.005)
 1026 [2004.08.005](https://doi.org/10.1016/j.agrformet.2004.08.005).
- 1027 Swenson, S., Chambers, D., & Wahr, J. (2008). Estimating geocenter varia-
 1028 tions from a combination of GRACE and ocean model output. *Journal of*
 1029 *Geophysical Research*, *113*, B08410. doi:[10.1029/2007JB005338](https://doi.org/10.1029/2007JB005338).
- 1030 Swenson, S., & Wahr, J. (2002). Methods for inferring regional surface-
 1031 mass anomalies from Gravity Recovery and Climate Experiment (GRACE)
 1032 measurements of time-variable gravity. *Journal of Geophysical Research*,
 1033 *107*, 2193. doi:[10.1029/2001JB000576](https://doi.org/10.1029/2001JB000576).

- 1034 Swenson, S., & Wahr, J. (2006). Post-processing removal of correlated errors
1035 in GRACE data. *Geophysical Research Letters*, *33*, L08402. doi:[10.1029/
1036 2005GL025285](https://doi.org/10.1029/2005GL025285).
- 1037 Tanaka, M., Adjadeh, T., Tanaka, S., & Sugimura, T. (2002). Water sur-
1038 face area measurement of Lake Volta using SSM/I 37-GHz polarization
1039 difference in rainy season. *Advances in Space Research*, *30*, 25012504.
1040 doi:[10.1016/S0273-1177\(02\)80320-9](https://doi.org/10.1016/S0273-1177(02)80320-9).
- 1041 Tapley, B. D., Bettadpur, S., Ries, J. C., Thompson, P. F., & Watkins, M. M.
1042 (2004). GRACE measurements of mass variability in the Earth system.
1043 *Science*, *305*, 503–505. doi:[10.1126/science.1099192](https://doi.org/10.1126/science.1099192).
- 1044 Taylor, J. C., van de Giesen, N., & Steenhuis, T. S. (2006). West Africa:
1045 Volta discharge data quality assessment and use. *Journal of the American
1046 Water Resources Association*, *42*, 1113–1126. doi:[10.1111/j.1752-1688.
1047 2006.tb04517.x](https://doi.org/10.1111/j.1752-1688.2006.tb04517.x).
- 1048 Taylor, K. E. (2001). Summarizing multiple aspects of model performance
1049 in a single diagram. *Journal of Geophysical Research*, *106*, 71837192.
1050 doi:[10.1029/2000JD900719](https://doi.org/10.1029/2000JD900719).
- 1051 Thiemiig, V., Rojas, R., Zambrano-Bigiarini, M., Levizzani, V., & De Roo, A.
1052 (2012). Validation of satellite-based precipitation products over sparsely
1053 gauged African River Basins. *Journal of Hydrometeorology*, *13*, 1760–1783.
1054 doi:[10.1175/JHM-D-12-032.1](https://doi.org/10.1175/JHM-D-12-032.1).
- 1055 Thiemiig, V., Rojas, R., Zambrano-Bigiarini, M., & Roo, A. D. (2013). Hy-
1056 drological evaluation of satellite-based rainfall estimates over the Volta and

- 1057 Baro-Akobo Basin. *Journal of Hydrology*, 499, 324–338. doi:[10.1016/j.](https://doi.org/10.1016/j.jhydrol.2013.07.012)
1058 [jhydrol.2013.07.012](https://doi.org/10.1016/j.jhydrol.2013.07.012).
- 1059 Velicogna, I., Tong, J., Zhang, T., & Kimball, J. S. (2012). Increasing sub-
1060 surface water storage in discontinuous permafrost areas of the Lena River
1061 basin, Eurasia, detected from GRACE. *Geophysical Research Letters*, 39,
1062 L09403. doi:[10.1029/2012GL051623](https://doi.org/10.1029/2012GL051623).
- 1063 Wahr, J., Molenaar, M., & Bryan, F. (1998). Time variability of the Earth's
1064 gravity field: Hydrological and oceanic effects and their possible detec-
1065 tion using GRACE. *Journal of Geophysical Research*, 103, 30,205–30,229.
1066 doi:[10.1029/98JB02844](https://doi.org/10.1029/98JB02844).
- 1067 Wahr, J., Swenson, S., & Velicogna, I. (2006). Accuracy of GRACE
1068 mass estimates. *Geophysical Research Letters*, 33, L06401. doi:[10.1029/](https://doi.org/10.1029/2005GL025305)
1069 [2005GL025305](https://doi.org/10.1029/2005GL025305).
- 1070 Werth, S., Güntner, A., Schmidt, R., & Kusche, J. (2009). Evaluation of
1071 GRACE filter tools from a hydrological perspective. *Geophysical Journal*
1072 *International*, 179, 1499–1515. doi:[10.1111/j.1365-246X.2009.04355.](https://doi.org/10.1111/j.1365-246X.2009.04355.x)
1073 [x](https://doi.org/10.1111/j.1365-246X.2009.04355.x).
- 1074 Xie, H., Longuevergne, L., Ringler, C., & Scanlon, B. (2012). Calibration and
1075 evaluation of a semi-distributed watershed model of sub-Saharan Africa
1076 using GRACE data. *Hydrology and Earth System Sciences Discussions*,
1077 9, 2071–2120. doi:[10.5194/hessd-9-2071-2012](https://doi.org/10.5194/hessd-9-2071-2012).
- 1078 Xue, B.-L., Wang, L., Li, X., Yang, K., Chen, D., & Sun, L. (2013). Evalu-
1079 ation of evapotranspiration estimates for two river basins on the Tibetan

- 1080 Plateau by a water balance method. *Journal of Hydrology*, 492, 290–297.
1081 doi:[10.1016/j.jhydrol.2013.04.005](https://doi.org/10.1016/j.jhydrol.2013.04.005).
- 1082 Yirdaw, S., Snelgrove, K., & Agboma, C. (2008). GRACE satellite ob-
1083 servations of terrestrial moisture changes for drought characterization in
1084 the Canadian Prairie. *Journal of Hydrology*, 356, 84–92. doi:[10.1016/j.jhydrol.2008.04.004](https://doi.org/10.1016/j.jhydrol.2008.04.004).
- 1086 Zeng, Z., Wang, T., Zhou, F., Ciais, P., Mao, J., Shi, X., & Piao, S. (2014).
1087 A worldwide analysis of spatiotemporal changes in water balance-based
1088 evapotranspiration from 1982 to 2009. *Journal of Geophysical Research:*
1089 *Atmospheres*, 119, 1186–1202. doi:[10.1002/2013JD020941](https://doi.org/10.1002/2013JD020941).
- 1090 van Zwieten, P., Béné, C., Kolding, J., Brummett, R., & Valbo-Jørgensen, J.
1091 (2011). *Review of tropical reservoirs and their fisheries – The cases of Lake*
1092 *Nasser, Lake Volta and Indo-Gangetic Basin reservoirs*. Technical Re-
1093 port 557 Food and Agriculture Organization of the United Nations Rome.
1094 URL: <http://www.fao.org/docrep/015/i1969e/i1969e.pdf> FAO Fish-
1095 eries and Aquaculture Technical Paper.

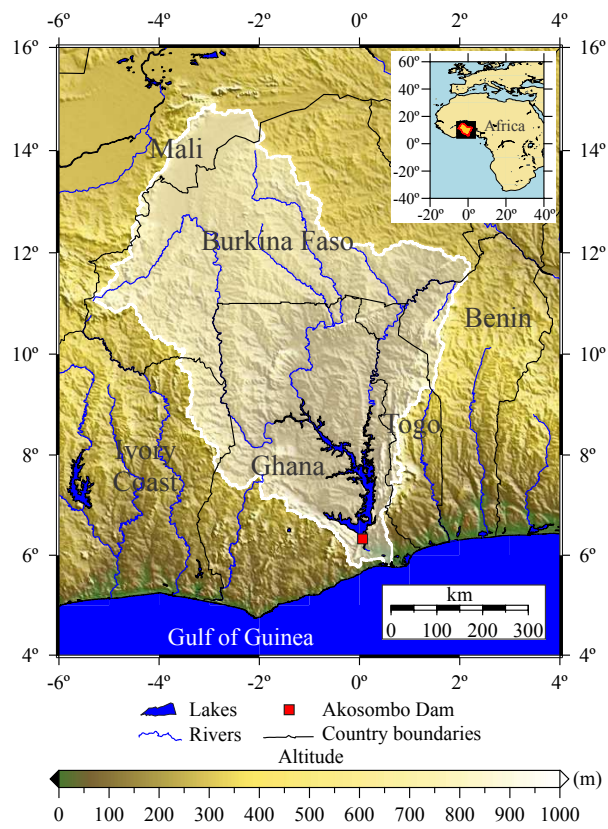


Figure 1: The Volta River Basin (shaded portion with an area of approximately 417,382 km²) and its riparian countries in West Africa. The scale is related to the parallel 10° N.

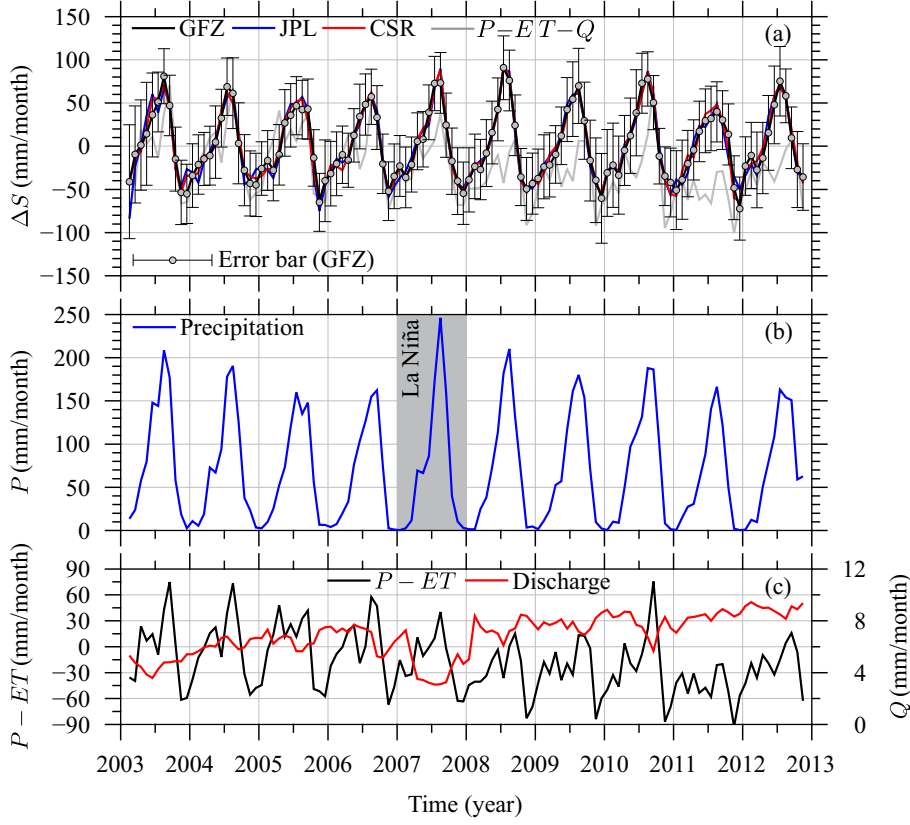


Figure 2: (a) Monthly Gravity Recovery and Climate Experiment (GRACE)-derived water-storage changes (ΔS) from the three different processing centers (Center for Space Research (CSR), Jet Propulsion Laboratory (JPL), *GeoForschungsZentrum* (GFZ)) and as a residual from $P - ET - Q$ using ERA-Interim reanalysis and river discharge data. (b) Tropical Rainfall Measurement Mission (TRMM) precipitation; the gray rectangle shows the La Niña event in 2007. (c) $P - ET$ by using ERA-interim, and *in-situ* discharge data.

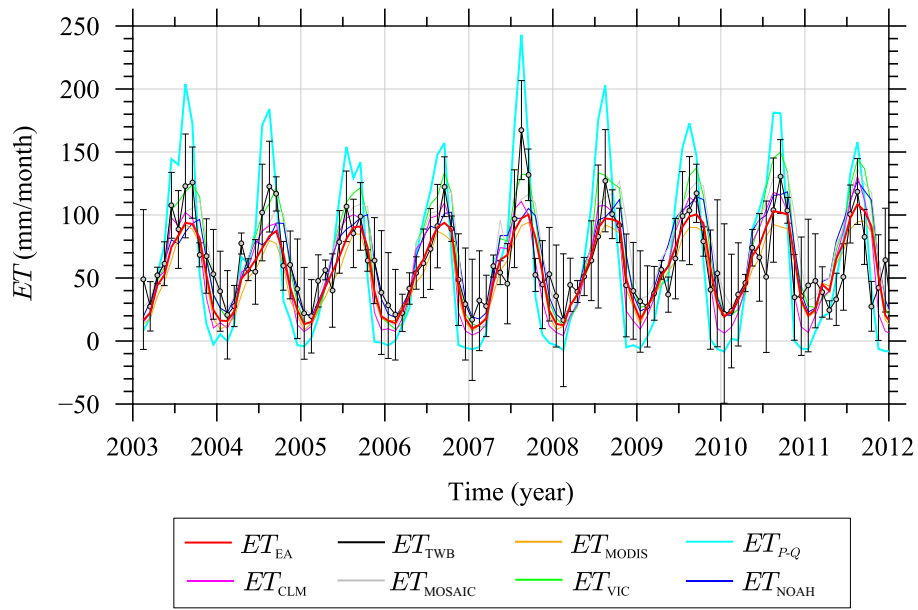


Figure 3: Monthly evapotranspiration from four versions of Global Land Data Assimilation System (GLDAS) (CLM, MOSAIC, NOAH and VIC) and those estimated by MODIS, GRACE, ensemble average and $P - Q$ over Volta Basin.

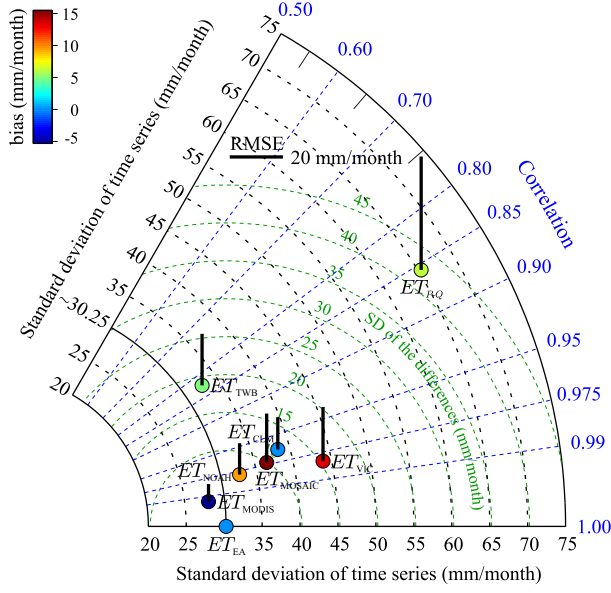


Figure 4: Taylor's diagram of statistical comparison between the time series of ensemble average ET (Ref.) and MODIS as well as GLDAS (VIC, NOAH, MOSAIC and CLM) and TWB-based.

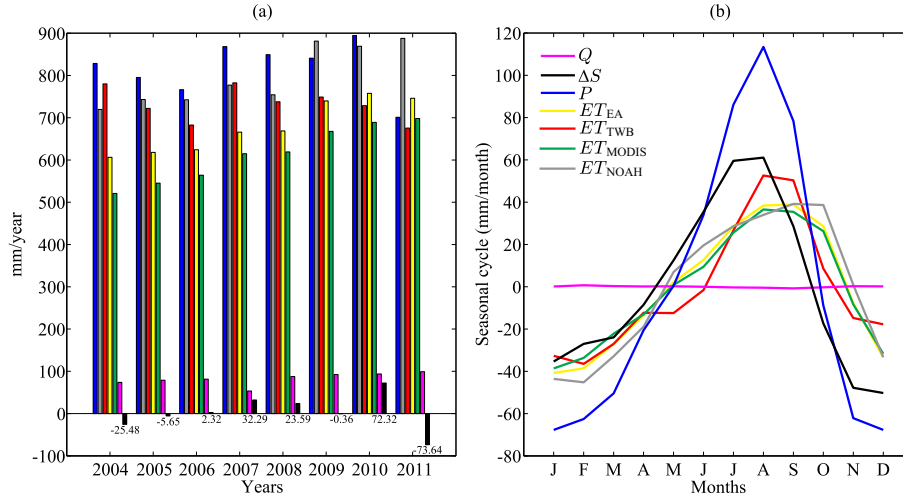


Figure 5: (a) Annual, basin averaged, totals of different ET products and the hydrological quantities $P-E$, Q , ΔS and P . (b) Mean annual cycle (using the calendar year) of different ET products and the hydrological quantities Q , ΔS and P for the period 2004-2011.

Table 1: Coefficients for least squares best fit over the time window of February 2003 to November 2012 at 95% confidence level.

Variable	Trend (mm/month/year)	Amplitude (mm/month)		Phase ($^{\circ}$)	
		Annual	Semi-annual	Annual	Semi-annual
ΔS	-0.00 ± 0.37	50.6 ± 1.5	18.2 ± 1.5	-167.8 ± 1.7	76.0 ± 4.7
ΔS^*	-4.49 ± 0.70	29.5 ± 2.8	22.8 ± 2.8	-171.0 ± 5.5	133.4 ± 7.1
P	-0.49 ± 0.60	84.3 ± 2.4	26.3 ± 2.4	-152.1 ± 1.6	95.5 ± 5.3
$P - ET$	-4.10 ± 0.70	29.1 ± 2.8	22.8 ± 2.8	-171.6 ± 5.5	133.4 ± 7.1
Q	0.39 ± 0.04	0.5 ± 0.1	0.1 ± 0.1	46.4 ± 17.8	-37.0 ± 131.7

Table 2: Statistical results over Volta Basin of MODIS, GLDAS (VIC, NOAH, MOSAIC and CLM), GRACE-derived and $P - Q$ (precipitation minus discharge) compared with ensemble average.

		Summary			
Model		R	SD	bias	RMSE
		(mm/month)			
ET_{TWB}		0.82	18.85	4.86	19.39
ET_{MODIS}		0.99	3.99	-5.30	6.63
GLDAS	ET_{VIC}	0.98	15.40	13.42	20.38
	ET_{NOAH}	0.98	7.06	9.44	11.77
	ET_{MOSAIC}	0.97	9.97	15.51	18.41
	ET_{CLM}	0.96	12.22	0.05	12.16
ET_{P-Q}		0.86	42.47	6.15	42.73